Oxygen isotope composition of evapotranspiration and its relation to C_4 photosynthetic discrimination

T. J. Griffis,[1] X. Lee,[2] J. M. Baker,[3] K. Billmark,[1] N. Schultz,[1] M. Erickson,[1] X. Zhang,[2] J. Fassbinder,[1] W. Xiao,[4] and N. Hu[4]

Received 7 August 2010; revised 13 December 2010; accepted 14 January 2011; published 23 March 2011.

[1] The oxygen isotope of water (^{18}O-H_2O) and carbon dioxide (^{18}O-CO_2) is an important signal of global change and can provide constraints on the coupled carbon-water cycle. Here, simultaneous observations of ^{18}O-H_2O (liquid and vapor phases) and ^{18}O-CO_2 were used to investigate the relation between canopy leaf water ^{18}O enrichment, ^{18}O-CO_2 photosynthetic discrimination ($^{18}\Delta$), isotope disequilibrium (D_{eq}), and the biophysical factors that control their temporal variability in a C_4 (*Zea mays L.*) ecosystem. Data and analyses are presented from a 74 day experiment conducted in Minnesota during summer 2009. Eddy covariance observations indicate that the oxygen isotope composition of C_4 evapotranspiration (δ_E) ranged from about −20‰ (VSMOW scale) in the early morning to −5‰ after midday. These values were used to estimate the isotope composition at the sites of leaf water evaporation ($\delta_{L,e}$) assuming non-steady-state conditions and revealed a strong diurnal pattern ranging from about −5‰ in the early morning to +10‰ after midday. With the addition of net ecosystem CO_2 exchange measurements and carbonic anhydrase (CA) assays, we derived canopy-scale $^{18}\Delta$. These estimates typically varied from 11.3 to 27.5‰ (VPDB scale) and were shown to vary significantly depending on the steady state or non-steady-state assumptions related to leaf water enrichment. We demonstrate that the impact of turbulence on kinetic fractionation and steady state assumptions result in larger estimates of $^{18}\Delta$ and D_{eq}. Further, the results indicate that both leaf-scale and canopy-scale CO_2 hydration efficiency may be substantially lower than that previously reported for laboratory conditions. These results may have important implications for interpreting variations in atmospheric ^{18}O-CO_2 and constraining regional carbon budgets based on the oxygen isotope tracer approach.

Citation: Griffis, T. J., X. Lee, J. M. Baker, K. Billmark, N. Schultz, M. Erickson, X. Zhang, J. Fassbinder, W. Xiao, and N. Hu (2011), Oxygen isotope composition of evapotranspiration and its relation to C_4 photosynthetic discrimination, *J. Geophys. Res.*, *116*, G01035, doi:10.1029/2010JG001514.

1. Introduction

[2] The oxygen isotope composition of CO_2 (^{18}O-CO_2) has long been viewed as a valuable tracer for disentangling the net CO_2 flux into its gross components, understanding the influences of land use change on the atmosphere, and inferring regional CO_2 sink/source strength [*Farquhar et al.*, 1993; *Yakir and Sternberg*, 2000; *Ishizawa et al.*, 2002; *Cuntz et al.*, 2003a, 2003b; *Riley et al.*, 2002, 2003; *Yakir*, 2003; *Ogée et al.*, 2004]. *Farquhar et al.* [1993] demonstrated the potential of using the ^{18}O-CO_2 tracer, showing that the spatial variation of ^{18}O-CO_2 photosynthetic discrimination ($^{18}\Delta$) was significant and that it could be used to help constrain the CO_2 sink strength between the terrestrial biosphere and ocean and to infer regional carbon sinks/sources on land. Recent advances in using the ^{18}O-CO_2 tracer, however, have been limited by three factors: First, there has been a lack of suitable technologies for measuring the ^{18}O-CO_2 flux; Second, given the coupling between ^{18}O-CO_2 and liquid water, via the ^{18}O isotope exchange during CO_2 hydration [*Mills and Urey*, 1940], interpretation of ^{18}O-CO_2 fluxes requires detailed information about the isotope composition of water pools and fluxes; Third, it remains unclear how the carbonic anhydrase (CA) enzyme influences the CO_2 hydration in the soil and in canopy leaves, which is important for accurate interpretation of the atmospheric ^{18}O-CO_2 signal [*Yakir*, 2003; *Seibt et al.*, 2006; *Cousins et al.*, 2008; *Wingate et al.*, 2009].

[3] *Gillon and Yakir* [2001] have shown that the ^{18}O enrichment of CO_2 in leaves varies among C_3 and C_4 species

[1]Department of Soil, Water, and Climate, University of Minnesota, Saint Paul, Minnesota, USA.
[2]School of Forestry and Environmental Studies, Yale University, New Haven, Connecticut, USA.
[3]Agricultural Research Service, U.S. Department of Agriculture, Saint Paul, Minnesota, USA.
[4]School of Applied Meteorology, Nanjing University of Information Science and Technology, Nanjing, China.

0148-0227/11/2010JG001514

due to differences in CA activity. Given similar environmental conditions, a high CA activity should increase the proportion of CO_2 that is in equilibrium with H_2O. A broad survey of CO_2 hydration efficiency in leaves ($\theta_{eq,leaf}$) indicates that values range from 0.93 for C_3 trees, 0.70 for C_3 grasses, and about 0.4 for C_4 species [*Yakir*, 2003]. A recent study by *Wingate et al.* [2009] suggests that CA activity in soils can also significantly accelerate soil CO_2 hydration to the extent that when accounted for in global models, the simulations agree better with flask network observations of ^{18}O-CO_2. However, recent measurement and modeling at the canopy scale suggests that the CO_2 hydration efficiency for C_3 ecosystems may be significantly lower than that observed for leaves in the laboratory or the values that are now prescribed in most models [*Xiao et al.*, 2010].

[4] The use of carbon and oxygen isotope tracers for partitioning net ecosystem fluxes and providing constraints on regional carbon sinks/sources depends strongly on the extent of isotope disequilibrium ($D_{eq} = |\delta_R - (\delta_a - {}^{18}\Delta)|$, the difference between the isotope composition of ecosystem respiration and photosynthesis). We have demonstrated in a C_3/C_4 (soybean/corn) rotation system that the ^{13}C-CO_2 isotope composition of ecosystem respiration equilibrates rapidly toward the recently fixed CO_2 from C_4 photosynthesis and that D_{eq} can become very small (≈0.5‰) by mid growing season [*Griffis et al.*, 2005b; *Zhang et al.*, 2006]. Further, others have shown that D_{eq} is very small (≈0.5‰) in undisturbed forests, which can limit the reliability of isotope flux partitioning [*Zobitz et al.*, 2008]. It has been suggested that the D_{eq} for ^{18}O-CO_2 should be significantly larger because of the strong difference in isotope composition of soil and plant leaf water [*Yakir and Wang*, 1996; *Yakir and Sternberg*, 2000; *Ogée et al.*, 2004]. Yet to date, only a few studies have measured the extent of ^{18}O-CO_2 D_{eq} under field conditions [*Wingate et al.*, 2010; *Seibt et al.*, 2006]. Recently, *Wingate et al.* [2010] reported near continuous and high frequency D_{eq} values for a forest site near Bordeaux, France using branch and soil chamber techniques. They demonstrated that D_{eq} was typically about 10‰, but diminished significantly following precipitation events.

[5] Of particular interest to carbon cycle studies that use the ^{18}O-CO_2 tracer is the need to determine the isotope composition of leaf water at the sites of evaporation ($\delta_{L,e}$) [*Welp et al.*, 2008]. This parameter represents a critical boundary condition for determining $^{18}\Delta$, but cannot be measured directly. A number of approaches have been proposed for estimating $\delta_{L,e}$ including the Craig-Gordon (CG) model by assuming steady state conditions [*Craig and Gordon*, 1965; *Dongmann et al.*, 1974; *Harwood et al.*, 1998; *Yakir and Sternberg*, 2000] and other methods that account for non-steady-state behavior and key processes such as leaf water turnover rate and the Péclet effect [*Farquhar and Lloyd*, 1993; *Lai et al.*, 2006a, 2006b; *Welp et al.*, 2008; *Farquhar and Cernusak*, 2005]. Measurements at the canopy scale are of particular importance because of the strong spatial variability observed in both stem and leaf water isotope ratios. For instance, our measurements indicate that the oxygen isotope composition of the bulk leaf water of corn leaves can vary by as much as 16‰ from petiole to leaf tip. Further, it remains unclear if leaf-level discrimination processes can be applied at the canopy scale [*Xiao et al.*, 2010].

[6] Measurements of ^{13}C-CO_2, ^{18}O-CO_2, and ^{18}O-H_2O are becoming more common under field conditions through the application of optical methods [*Bowling et al.*, 2003a; *Griffis et al.*, 2010a; *Lee et al.*, 2005; *Wen et al.*, 2008; *Welp et al.*, 2008; *Wang et al.*, 2009; *Wingate et al.*, 2010]. In this paper we examine the oxygen isotope composition of evapotranspiration and estimate $\delta_{L,e}$ from isotope water vapor flux measurements to provide new insights regarding the role of C_4 vegetation (corn) and its influence on ^{18}O-CO_2 exchange and the atmospheric budget of ^{18}O. While we are using C_4 corn as a model ecosystem we acknowledge that its leaf-level CO_2 hydration efficiency is more characteristic of C_3 grasses ($\theta_{eq,leaf} \approx 0.70$) [*Yakir*, 2003; *Affek et al.*, 2006].

[7] Figure 1 provides an overview of the key processes investigated in this paper and a summary of the typical values observed. Our investigation explores: meteorological factors that influence the boundary layer water vapor and its relation to leaf water enrichment (Figure 1, process A); biophysical processes that control leaf water enrichment and the oxygen isotope composition of photosynthetic CO_2 exchange (Figure 1, process B); and the isotope composition of soil respiration and its influence on ^{18}O-CO_2 disequilibrium (Figure 1, process C).

[8] To provide a better understanding of the biophysical factors that influence atmospheric variations in ^{18}O-H_2O and ^{18}O-CO_2, the following questions are pursued: (1) From a land use change perspective, can C_4 (*Zea mays L.*) be distinguished from C_3 (*Glycine max*) crops in terms of their influence on the isotope composition of evapotranspiration and net ecosystem CO_2 exchange (i.e., their isofluxes)? (2) Are leaf-level and canopy-scale estimates of CO_2 hydration efficiency significantly different between these two photosynthetic pathways? (3) Is the ^{18}O composition of CO_2 strongly coupled to the water isotope signal in C_4 ecosystems? (4) How strong is the ^{18}O-CO_2 isotope disequilibrium and what controls its temporal variability?

2. Basic Theory

[9] Photosynthesis imparts a major influence on the biosphere-atmosphere exchange of ^{18}O-CO_2 and is intimately related to transpiration and the isotope content at the evaporating sites in plants leaves. These mechanisms are relatively well known and the isotope composition at the site of leaf evaporation has been estimated using the Craig-Gordon (CG) model by assuming steady state conditions [*Yakir and Sternberg*, 2000; *Craig and Gordon*, 1965],

$$\delta_{L,s} = \delta_x + \epsilon_{eq} + \epsilon_k^w + h\left(\delta_v - \epsilon_k^w - \delta_x\right) \quad (1)$$

where $\delta_{L,s}$ is the isotope composition at the sites of evaporation assuming steady state conditions, δ_x is the isotope composition of the xylem water, h is the relative humidity (expressed as a fraction in reference to leaf temperature), δ_v is the isotope composition of the water vapor, ϵ_k^w is the kinetic fraction factor for $H_2^{18}O$, and ϵ_{eq} is the temperature-dependent equilibrium fractionation effect between liquid water and vapor [*Majoube*, 1971]. Here ϵ_k^w was calculated following *Lee et al.* [2009] to account for the important influence of atmospheric turbulence on kinetic fractionation in both water vapor and carbon dioxide.

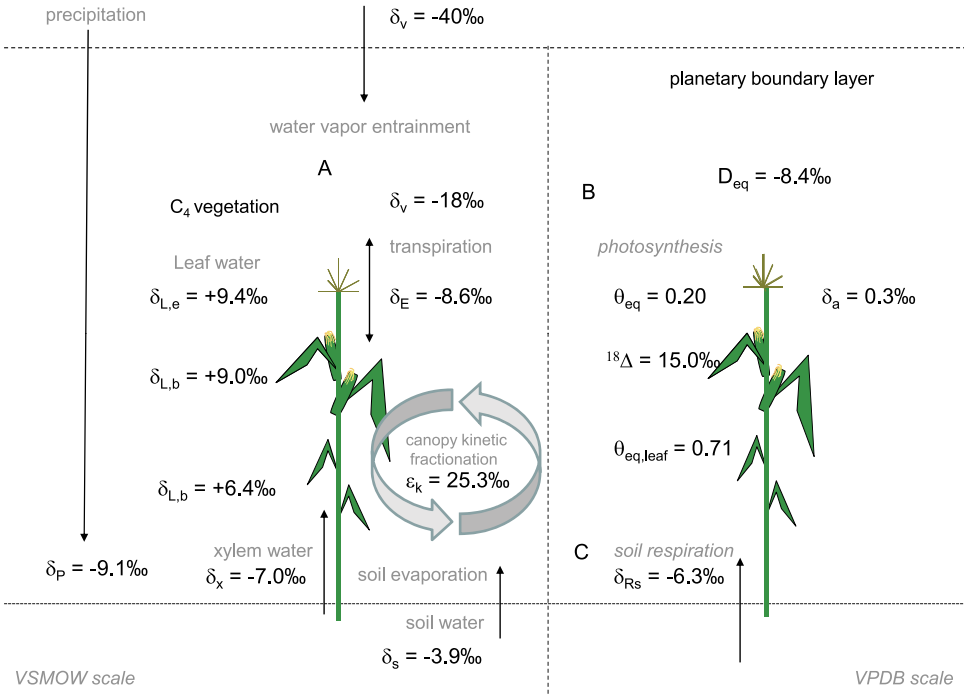

Figure 1. Overview of processes and representative oxygen isotope values observed near midday during the growing season for a C_4 corn canopy located in the upper Midwest, United States. The oxygen isotope ratio of water vapor above the planetary boundary layer is taken from *He and Smith* [1999].

[10] Numerous studies have demonstrated that the steady state condition is rarely met at subdaily timescales [*Dongmann et al.*, 1974; *Harwood et al.*, 1998; *Lee et al.*, 2007; *Welp et al.*, 2008]. *Welp et al.* [2008] used high-frequency water vapor isotope flux measurements over a soybean (C_3) canopy to estimate the non-steady-state isotope composition at the site of leaf evaporation ($\delta_{L,e}$) and the departure from steady state (i.e., the difference between $\delta_{L,s}$ and $\delta_{L,e}$). In this case the isotope composition of transpiration (δ_T) is substituted for δ_x in equation (1) and is approximated with the isotope composition of evapotranspiration ($\delta_E \approx \delta_T$). Determining $\delta_{L,e}$ is challenging, but crucial for understanding the ^{18}O signal in CO_2. Here, we combined eddy covariance and tunable diode laser spectroscopy to measure δ_E directly and to approximate δ_T [*Griffis et al.*, 2010b].

[11] As CO_2 diffuses through the stoma and goes into solution at the chloroplast it isotopically equilibrates according to the temperature-dependent CO_2 hydration reaction [*Hesterburg and Siegenthaler*, 1991],

$$\begin{aligned} H_2^{18}O(l) + CO_2(g) &\longleftrightarrow H^+ + \left[HCO_2^{18}O\right]^-(aq) \\ &\longleftrightarrow H_2O(l) + CO^{18}O(g) \end{aligned} \tag{2}$$

The temperature dependence of this hydration reaction can be expressed as an equilibration factor (ϵ^c_{eq}) and is given by [*Brenninkmeijer et al.*, 1983],

$$\epsilon^c_{eq} = \frac{17604}{T} - 17.93 \tag{3}$$

where T is the temperature (K). The reaction expressed in equation (2) represents a relatively slow abiotic process, but is catalyzed by the CA enzyme found in leaves [*Gillon and Yakir*, 2000a, 2001] and soils [*Wingate et al.*, 2009, 2008].

[12] The ^{18}O-CO_2 photosynthetic fractionation ($^{18}\Delta$), based on the big-leaf analogy, can be described as [*Yakir*, 2003; *Xiao et al.*, 2010],

$$^{18}\Delta \approx \epsilon^c_k + \frac{C_c}{C_a - C_c}\left[\theta_{eq}\left(\delta^c_{L,e} - \delta_a\right) - \left(1-\theta_{eq}\right)\epsilon^c_k \Big/ \left(\frac{C_c}{C_a - C_c} + 1\right)\right] \tag{4}$$

where $\delta^c_{L,e} = \epsilon^c_{eq} + \delta_{L,e}$ (reported on the VPDB scale), ϵ^c_k is the kinetic fractionation factor for ^{18}O-CO_2, C_a and C_c represent the CO_2 concentration in the surface layer and the leaf chloroplast, the fraction ($\frac{C_c}{C_a - C_c}$) describes the retroflux of ^{18}O-CO_2, and θ_{eq} is the canopy-scale CO_2 hydration efficiency (ranging from 0 to 1 depending on species and photosynthetic pathway) and has been estimated at the leaf-level ($\theta_{eq,leaf}$) previously as [*Gillon and Yakir*, 2000b],

$$\theta_{eq,leaf} = 1 - e^{-k\tau/3} \tag{5}$$

where $k\tau = CA_{leaf}/F_{in}$ and where the gross flux, F_{in} was estimated from the product of the atmospheric CO_2 concentration and the total conductance to the site of CO_2-H_2O equilibration [*Gillon and Yakir*, 2000b].

[13] With direct observation of the isotope composition of the soil CO_2 efflux, measured here with automated soil chambers, the ^{18}O-CO_2 isoflux can be approximated as,

$$F_\delta = \left(\delta_a - {}^{18}\Delta\right)F_P + \delta_R F_R \tag{6}$$

where F_δ is the ^{18}O-CO_2 isoflux, δ_a is the oxygen isotope ratio of CO_2 in the surface layer, F_P, is gross photosynthesis, δ_R is the net isotope composition of the soil CO_2 efflux and includes the influence of both the soil respiration and the abiotic invasion flux [*Tans*, 1998; *Wingate et al.*, 2009], and F_R is ecosystem respiration. Here, F_P can be approximated using traditional micrometeorological techniques (i.e., $F_P = F_N - F_R$).

3. Methodology

3.1. Research Site and Background

[14] This study was conducted at the University of Minnesota's Rosemount Research and Outreach Center (RROC) from 19 June (DOY 170) to 31 August (DOY 243) 2009. A major storm hit the site on DOY 220 resulting in significant equipment damage and loss of data. For this reason some of the analyses are restricted to the period DOY 170 to DOY 220. The site is part of the AmeriFlux network and is currently managed in a conventional corn/soybean rotation. Net ecosystem CO_2 exchange (F_N) and the energy balance components have been measured near-continuously at this site since 2003. The measurements reported here were made during the corn (*Zea mays L.*, C_4 photosynthetic pathway) phase of the rotation. In addition to the traditional micrometeorological measurements we used an eddy covariance and water vapor tunable diode laser (EC-TDL) system to measure the isotope composition of evapotranspiration. This system was located approximately 50 m from the northern edge of the research field. Southerly winds produce an upwind fetch of about 350 m. The TDL was operated in the field and was located about 1.5 m from the tower. A very similar micrometeorological setup was used in 2006 at the same field site and the details have been reported elsewhere [*Griffis et al.*, 2008; *Welp et al.*, 2008; *Lee et al.*, 2009; *Xiao et al.*, 2010].

3.2. Water Isotope Measurements

[15] Water vapor isotope mixing ratios ($H_2^{16}O$, $H_2^{18}O$ and HDO) were measured at 10 Hz using a TDL system (TGA200, Campbell Scientific Inc., Logan, Utah, USA). Here we focus our attention on $H_2^{16}O$ and $H_2^{18}O$, and their ratio ($\delta^{18}O$), and the relation to ^{18}O-CO_2. In this experiment $H_2^{16}O$ and $H_2^{18}O$ absorption were measured at wave numbers of 1500.546 cm^{-1} and 1501.188 cm^{-1}, respectively [*Griffis et al.*, 2010b].

[16] Liquid water, including precipitation, xylem, leaf, soil water, and the water used for calibration of the TDL, were analyzed using a distributed feedback (DFB, near-infrared) TDL with off-axis integrated-cavity-output spectroscopy (DLT-100, Los Gatos Research Inc., Mountain View, California) [*Lis et al.*, 2008; *Griffis et al.*, 2010b].

[17] Xylem, leaf and soil water were extracted on a custom designed glass vacuum line. All water isotope analyses were conducted by running each sample 6 times to reduce memory effects. We rejected the first three measurements and used the final three measurements to characterize the isotope ratio of each sample. For each run, water standards were chosen to bracket the expected values for that set of unknown samples. In some cases, samples were reanalyzed to provide an optimal set of calibration standards. Typical precision was 0.2‰ for $\delta^{18}O$.

[18] We followed the sampling protocol proposed by the Moisture Isotopes in the Biosphere and Atmosphere program for xylem, leaf and soil water sampling (http://www-naweb.iaea.org/napc/ih/IHS_resources_miba.html). Briefly, xylem, leaf (top leaf of canopy and bottom leaf of canopy), and soil (10 cm depth) were collected near midday (1200 LST). Leaf samples were only collected for dry canopy conditions. For corn, the main vein was removed and the leaf was cut in half-lengthwise. For soybean, the leaf vein was removed and the entire leaf was used for water extraction. The plant leaf and soil samples were sealed in glass vials, wrapped with paraffin, and frozen until cryogenic water extraction on the glass vacuum line.

3.3. Carbon Isotope Fluxes and Supporting Environmental Measurements

[19] A second TDL was used to measure ^{18}O-CO_2 and $C^{16}O_2$ (TGA100A, CSI) mixing ratios and gradients using the same micrometeorological tower described above. These measurements were used to quantify the ecosystem-scale ^{18}O-CO_2 isoflux and to perform the canopy-scale hydration efficiency optimization described later. The details related to the sampling, calibration procedure, and data quality control have been described in detail elsewhere [*Griffis et al.*, 2005b, 2007]. Finally, we used an automated chamber system (model ACS-DC, Biometeorology and Soil Physics Group, University of British Columbia, Vancouver, Canada) [*Gaumont-Guay et al.*, 2006; *Griffis et al.*, 2004] to measure soil evaporation and soil respiration directly. In this chamber system an equilibration tube (0.20 m) was used to prevent significant pressure differences between the chamber and atmosphere. Further, the long sample lines (20 m) connecting each of the chambers to the analytical instruments also acted to buffer these pressure differences.

[20] We integrated the automated chamber system with the carbon isotope TDL to determine the oxygen isotope composition of the soil respiration [*Fassbinder*, 2010]. The chamber sample tubing was heated using heating tape and wrapped in foam insulation to prevent condensation. In addition, the sample air pressure was reduced in order to lower the dew point temperature. Condensation on the chamber walls did occur. However, *Wingate et al.* [2010] examined this issue and concluded that the CO_2 equilibration time was too long relative to the sampling interval to have a significant influence on the measurement.

[21] The concentration change with time inside the chambers was determined using linear regression based on the first 30 s of data, but omitting 10 s of data following chamber closure. Soil evaporation and soil respiration were calculated from,

$$F_i = \frac{\rho_a V S}{A} + F_{cor} \tag{7}$$

where F_i represents the soil CO_2 or H_2O flux, ρ_a is the molar density of dry air, V is the air-filled volume (0.05 m^3) of the chamber corrected for temperature and pressure, S is the rate of change in mixing ratio (obtained from a regression analysis) of the scalar of interest (H_2O, ^{18}O-CO_2, and $C^{16}O_2$) and A represents the soil surface area enclosed by the chamber (0.22 m^2). Since the TDL analyzer does not return the sampled air back to the chamber, a balance of 0.25 L min^{-1}

of N_2 was injected into the chamber manifold to prevent a pressure perturbation. This had the effect of diluting the concentration change with time and underestimating the true flux. F_{cor} represents the flux correction for the soil evaporation and each isotope of CO_2. For example, the $C^{16}O_2$ flux was typically underestimated by 0.21 μmol m^{-2} s^{-1} and the median isotope ratio correction to the flux was +0.3‰ (i.e., enrichment). The correction factor was estimated by multiplying the mean mixing ratio of the scalar of interest by the sample flow rate during each chamber measurement. The oxygen isotope composition of the soil CO_2 flux was determined from the ratio of the individual ^{18}O-CO_2 and $C^{16}O_2$ fluxes (flux ratio approach). The uncertainty in the soil ^{18}O-CO_2 flux ratio value was typically 1.3‰, which is slightly larger than that reported by *Wingate et al.* [2010] for soil and leaf chambers coupled to a TDL system (TGA100A, CSI).

[22] We acknowledge that the chamber measurement of soil evaporation represents a lower estimate of the true value due to the strong impact of chamber closure on the available energy, turbulence, vapor pressure deficit, etc. However, the measured values are in relatively good agreement with those estimated using the Shuttleworth and Wallace model for the same site during the corn phase of the rotation [*Zhang et al.*, 2006].

[23] In this study F_N was measured using a 3-D sonic anemometer-thermometer (CSAT3, CSI) and an open-path infrared gas analyzer (LI-7500, Licor Inc., NB, USA). All eddy fluxes were obtained from 30 min block averaging followed by two-dimensional coordinate rotation [*Baker and Griffis*, 2005]. Canopy temperature (T_c) was measured using an infrared thermometer (model IRTS-P and SI-111, Apogee Instruments Inc., Utah, USA). Leaf wetness (L_w), above and within the canopy, was measured with dielectric wetness sensors (Leaf Wetness Sensor, Decagon Devices, Pullman WA). Precipitation was measured using a weighing gauge (6021 Series Electrically Heated Rain and Snow Gauge, Qualimetrics, AllWeatherInc., Sacramento, CA, USA). Air temperature (T_a) and relative humidity (h) were measured at 3.2 m above the ground surface (HMP35C, Vaisala, Woburn, MA).

3.4. Carbonic Anhydrase Assays

[24] Carbonic anhydrase (CA) extracts were prepared according to the methodology presented by *Makino et al.* [1992]. Briefly, leaf subsamples were ground with a chilled mortar and pestle in approximately 1 mL of extraction buffer per square centimeter of leaf subsample. The extraction buffer consisted of 50mM HEPES-NaOH at a pH of 8.3, 0.5mM EDTA, 10mM dithiothreitol, 10% (v/v) glycerol, and 1% (v/v) Triton X-100. The samples were then spun at 5,000 rpm for 10 min, following which the supernatant was decanted into a vial and frozen at −20°C until assayed. The assay was performed on 20 μL of sample extract added to 3 mL of assay buffer (20 mM Na-barbitol at pH 8.3). The assay was started by adding 1 mL of distilled water saturated with CO_2 at 0°C. The activity was determined as the rate of change from pH 8.3 to 7.3. The molar rate of equivalent CO_2 hydrated was determined by titrating the extract and assay buffer through the same pH change with 0.2 N H_2SO_4 [*Hatch and Burnell*, 1990], where the resultant activity, CA_{assay}, expressed as μmol CO_2 hydrated m^{-2} s^{-1}, represents the activity at assay temperature (2°C). An equivalent activity at leaf temperature was determined by applying Henry's Law to the CO_2 concentration at the chloroplast surface (c_c) at measured leaf temperatures, assuming that the concentration at half maximal activity (K_m) is equal to 2.5 mM and correcting for leaf temperature by assuming $Q_{10} = 2$ [*Hatch and Burnell*, 1990]. The c_c was estimated from Fick's Law assuming an internal conductance to c_c of 1 mol m^{-2} s^{-1} [*Gillon and Yakir*, 2001]. Leaf-level CO_2 exchange was measured in the field using a dynamic leaf chamber (LI-6400, Licor Inc., Lincoln, NB). We note that these measurements were not performed simultaneously on the same leaves. Finally, the extent of isotope equilibrium between CO_2 and H_2O was estimated as $\theta_{eq,leaf} = 1 - e^{-k\tau/3}$. All samples were taken on 31 August and 1 September 2009 at 1200 LST.

3.5. Numerical Optimization of Canopy-Scale Hydration Efficiency

[25] Daytime (0500–1800 LST) ensemble values of the variables (F_δ, F_P, C_c, C_a, $\delta^c_{L,e}$, δ_a, ϵ_k) in equations (4) and (6) and a nonlinear optimization method were used to constrain θ_{eq} independent of the leaf-level CA assays. Variables measured directly included C_a, and δ_a, while the remaining variables were derived from well known biophysical functions and supporting measurements. For example, C_c was derived from canopy-scale conductance measurements based on the Penman-Monteith combination equation and estimates of canopy-scale photosynthesis. The ecosystem-scale isoflux (F_δ) was calculated as the product of net ecosystem CO_2 exchange and its isotope composition determined from the flux ratio approach [*Griffis et al.*, 2005b]. The Nelder-Mead simplex (direct search) optimization routine (Matlab, V8, The Mathworks Inc., USA), with an initial parameter value of 0.5 was specified for θ_{eq} without constraining the upper or lower bounds.

4. Results and Discussion

4.1. Climatology and Phenology

[26] The 2009 growing season was colder than normal (Table 1). Precipitation and dew point temperatures were significantly lower during May through July, while August was much wetter than normal. September returned to drier and warmer conditions. Canopy height and LAI reached a maximum of 2.7 m and 6.4 on DOY 218 (6 August). Wind speed measurements above the canopy indicate substantially lower mean velocities during June, July, and August of 2009 compared to over soybean 2008. Wind speed was similar or slightly lower than over soybean in 2006. This observation is directly related to the taller vegetation (corn) and the increased aerodynamic roughness and has particular relevance here because of its influence on kinetic fractionation of ^{18}O-H_2O and ^{18}O-CO_2 [*Lee et al.*, 2009].

[27] As noted by *Welp et al.* [2008] the frequency of dew at this site is relatively high and has a significant influence on the isotope exchange of water vapor. Leaf wetness sensors mounted above and within the canopy showed that the upper canopy leaves were wet more frequently (i.e., 31% of the total half-hourly observations) than within canopy leaves (16% of the total half-hourly observations). The ensemble diurnal pattern of leaf wetness (not shown) revealed that the

Table 1. Climate and Phenology[a]

Month	T_a (°C)	T_d (°C)	h	Precipitation (cm)	Wind Speed (m s^{-1})	LAI (m^2 m^{-2})	h_c (m)
May 2008	12.6 (−1.6)	4.0 (−3.3)	0.55	8.4 (−1.6)	2.9	-	-
Jun 2008	19.0 (−0.4)	11.5 (−2.0)	0.61	10.5 (−1.0)	2.7	0.13	0.079
Jul 2008	22.2 (+0.5)	14.9 (−1.5)	0.63	7.0 (−4.7)	2.1	2.3	0.37
Aug 2008	20.7 (+0.4)	14.2 (−1.5)	0.66	7.6 (−4.0)	1.5	4.1	0.78
Sep 2008	16.9 (+1.4)	11.3 (+0.4)	0.69	5.7 (−3.1)	2.5	1.0	-
May 2009	13.9 (−0.3)	3.3 (−4.0)	0.48	3.4 (−6.7)	3.6	-	-
Jun 2009	18.2 (−1.2)	10.5 (−3.0)	0.60	9.8 (−1.7)	1.8	0.59	0.4
Jul 2009	19.0 (−2.7)	11.7 (−4.7)	0.62	4.7 (−7.0)	1.5	3.5	2.0
Aug 2009	19.6 (−0.7)	13.3 (−2.4)	0.67	19.5 (+7.9)	1.3	5.6	2.6
Sep 2009	17.7 (+2.2)	11.9 (+1.0)	0.68	1.5 (−7.3)	0.9	3.8	2.6

[a]Parentheses indicate the departure from the 30 year climate normal (1971–2000) except for dew point temperature where parentheses indicate the most recent 25 years. Here, relative humidity was calculated from the T_a and T_d values presented above in Table 1.

top leaves have higher wetness duration at night and that they dry out before the within canopy leaves. The whole-canopy on a typical day can be considered "dry" from about 1100 to 2000 LST. Such patterns have important implications for the canopy-air exchange of isotope water vapor and leaf water isotope ratios (described later).

[28] During the 2009 growing season water vapor mixing ratios (χ_w) ranged from about 9.5 to 30 mmol mol^{-1} (Figure 2). The half-hourly δ_v values ranged from about −32‰ to about −8‰. For southerly flow, the log linear relation between δ_v and χ_w showed an expected decrease in δ_v as mixing ratio decreased ($\delta_v = 9.1 \ln(\chi_w) - 43.1$, $r^2 = 0.49$). This result is qualitatively similar with other investigations conducted at the same site during 2006 and over a forest site and coastal site near New Haven Connecticut [*Welp et al.*, 2008; *Lee et al.*, 2006, 2007]. In general, warm southerly flow resulted in higher water vapor mixing ratios that were isotopically more enriched, a consequence of the air mass back trajectory and its condensation history. Synoptic meteorological conditions, therefore, exert an important influence on δ_v and indirectly on $\delta_{L,e}$ and $^{18}\Delta$ (see sensitivity analysis described later). With southerly flow, the isotope composition of the leaf water can be expected to adjust toward a more enriched δ_v value, especially as h approaches unity.

4.2. Oxygen Isotope Composition of Water Pools

[29] Tracking the variations in the isotope composition of precipitation (δ_P) is critical as it effectively resets the boundary condition of the plant source water. The seasonal amplitude of δ_P is large, with values ranging from about −30 to 0‰ from winter to summer, respectively. The strong seasonality can be attributed to changes in storm tracks and to Rayleigh distillation effects [*Welker*, 2000].

[30] Here we contrast the differences in the isotope composition of the water pools for 2006/2008 (soybean) and 2009 (corn) to determine if there are any important intrinsic differences that could impact $^{18}\Delta$ and $^{18}O\text{-}CO_2$ exchange. The growing season δ_P (weighted by precipitation magnitude) in 2008 was −7.4‰ (Table 2). Analysis of the extracted bulk leaf water ($\delta_{L,b}$) from soybean during 2008 showed values ranging from about −1.5 to 26.7‰ with a mean midday value of 10.0‰ and 7.5‰, for the top and bottom leaves, respectively. Mean xylem (δ_x) and soil water (δ_s at 10 cm depth) were −5.5 and −3.3‰, respectively. In contrast, *Welp et al.* [2008] reported more enriched precipitation for 2006 with mean June–September values of −6.8‰, and more depleted xylem and soil water values of −6.5‰, and −6.3‰, respectively. During 2006, $\delta_{L,b}$ values ranged from a minimum of 0‰ to a maximum of 20‰ with significant diurnal variation (≈20‰ variation was observed on many days).

[31] In 2009 (corn) δ_P was very similar to May and August of 2008. Differences between June and July 2008/2009 were significant, indicating different source origins of the precipitation. Analysis of $\delta_{L,b}$ showed values ranging from about 0 to 17.3‰ with a midday mean of 8.3‰ and 5.8‰ for the bottom and top leaves, respectively.

[32] We hypothesized that the difference between δ_x and $\delta_{L,b}$ would be greater for corn than soybean because of the significant difference in canopy architecture. According to the analysis of *Lee et al.* [2009], the kinetic fractionation increases significantly for rougher surfaces (enhanced turbulent kinetic effect) when the canopy resistance is similar or lower than the aerodynamic resistance. In addition, the deeper rooting system of corn versus soybean implies that the isotope composition of the soil water should be more depleted under similar climatological and hydrological conditions. It was only during July (closed canopy) that this hypothesis was supported by the data. The mean difference between δ_x and $\delta_{L,b}$ for July was about +16‰ for corn and +13‰ for soybean.

[33] Using mean values for 2008 and 2009, we observed remarkable similarity of +15.4‰ (soybean, top leaf - xylem) versus +15.3‰ (corn, top leaf - xylem) and +12.9‰ (soybean, bottom leaf - xylem) and +12.8‰ (corn, bottom leaf - xylem). We suspect that this similarity is a consequence of the more depleted δ_v observed over the course of the 2009 growing season, which acted to lower the $\delta_{L,b}$ values. Unfortunately, δ_v observations from 2008 were too sporadic to test this conclusively.

[34] Canopy architecture also influences the vertical variation of $\delta_{L,b}$. For corn, a strong difference in $\delta_{L,b}$ was observed between the lower and upper leaves. These differences directly influence canopy $^{18}\Delta$, and further highlight the need for obtaining canopy-scale information about the fractionation processes. In June, the bottom leaves were relatively enriched by 3.2‰ compared to the top leaves. A reversal in pattern was observed later in the growing season (after DOY 200) that is consistent with canopy closure (Figure 3). A similar, but less pronounced, pattern was reported by *Welp et al.* [2008] for soybean. They hypothesized that the difference was directly related to changes in the

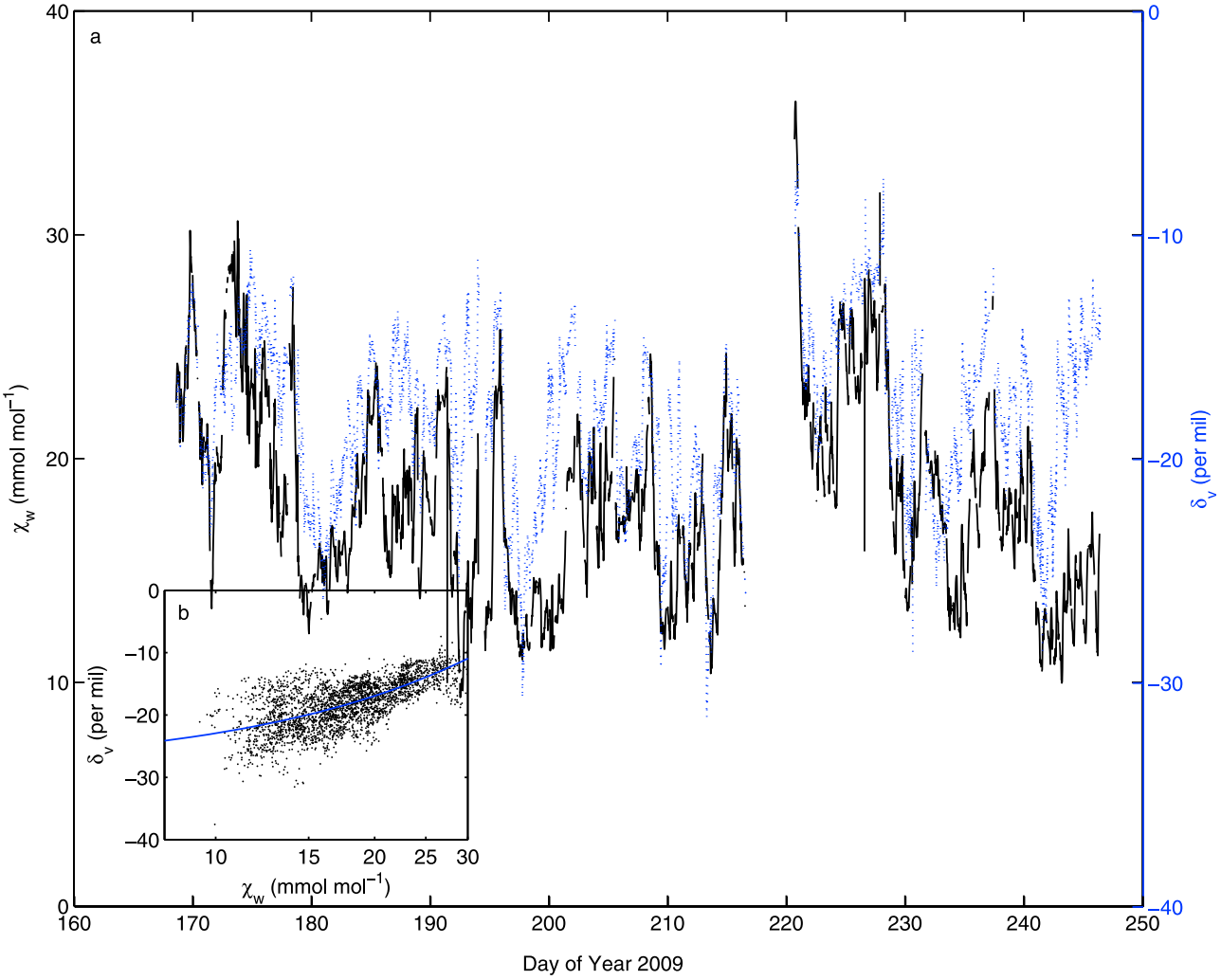

Figure 2. (a) Time series of water vapor mixing ratio (black line) and its oxygen isotope composition (dashed blue line) during the 2009 growing season. (b) The relation between water vapor mixing ratio and isotope composition.

canopy humidity profile as it adjusted to changes in canopy architecture. Higher values of h within the canopy after closure (LAI > 1) should cause the isotope ratio of the leaf water to tend toward the equilibrium value with the water vapor (typically a very depleted value). Further, the kinetic fractionation effect should be significantly different between the top and bottom leaves of the canopy depending explicitly on the ratio between the canopy and aerodynamic resistances. A multilayer canopy model is being adapted to help explore these processes in greater detail.

4.3. Isotope Composition of Evapotranspiration

[35] Here we quantified the isotope composition of evapotranspiration in order to help determine $\delta_{L,e}$ and to examine its relative importance on variations in δ_v. Evapotranspiration (F_E) during the 2009 growing season reached a mean maximum value of about 8 mmol m^{-2} s^{-1} with small negative values (condensation events), representing about 18% of the valid half-hourly eddy covariance data. On average, F_E was nearly equal to the estimated equilibrium evaporation rate indicating that the canopy was not significantly water stressed. Soil evaporation (F_s), measured with two automated chambers, showed a strong diurnal pattern with maximum values ranging up to about 1.5 mmol m^{-2} s^{-1}. Based on the ensemble diurnal pattern of F_E and F_s from DOY 170 to 210 (data not shown), daytime F_s was typically less than about 7% of F_E (i.e., when LAI > 1). These results are in excellent agreement with *Zhang et al.* [2006] who modeled soil evaporation at the same site during a corn year. Therefore, at full canopy, F_E represents a

Table 2. Oxygen Isotope Composition of Water Pools[a]

Month	Precipitation	Soil	Stem	Lower Leaf	Upper Leaf	Leaf Stem
Jun 2008	−7.3	−1.6	−3.5	NaN	12.3	15.8
Jul 2008	−7.5	−3.9	−6.1	4.8	6.8	12.9
Aug 2008	−5.4	−3.4	−6.0	10.2	12.9	18.9
Jun 2009	−5.6	−5.4	−7.4	8.5	5.3	12.7
Jul 2009	−9.1	−3.9	−7.0	6.4	9.0	16.0
Aug 2009	−5.6	−6.2	−6.5	3.0	9.1	15.6

[a]Note that 2008 and 2009 represent soybean and corn years, respectively. All values are given in ‰ in reference to VSMOW. Values for 2006 (soybean) are presented by *Welp et al.* [2008].

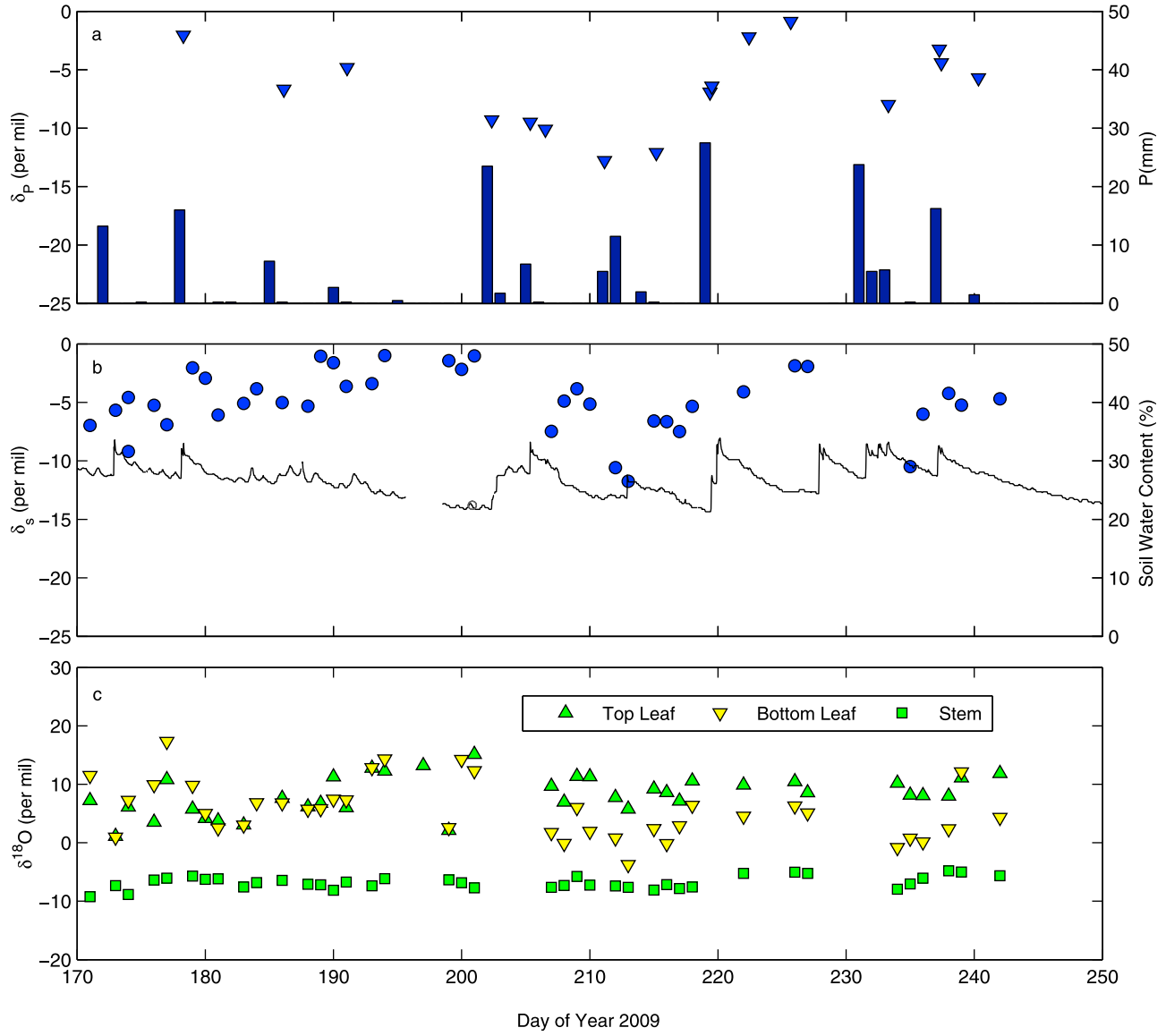

Figure 3. Seasonal variation in the isotope composition of liquid water including: (a) precipitation (amount is designated as bars, and isotope composition is shown as symbols); (b) soil water at a depth of 10 cm (water content is designated as a line, and isotope composition is shown as symbols); (c) midday stem (squares) and leaf water (triangles).

relatively good approximation of transpiration and $\delta_E \approx \delta_T$ [*Griffis et al.*, 2010b].

[36] Over longer timescales (days to weeks), mass balance requires that the isotope composition of the source water be equal to that being transpired back to the atmosphere. The mean δ_x for the measurement period was -7.0 ± 1.1‰. This value compared reasonably well with the flux-weighted δ_E for all half-hourly data (-7.7 ± 4.8‰), but δ_E was relatively depleted compared to the source (xylem) water. Three factors make it difficult to directly compare these values. First, xylem water sampling at midday may not adequately capture the temporal or spatial variation. Based on short intensive sampling campaigns we found the δ_x to vary by as much as 1.4‰ within a 24 h period. Similar variability has been reported in other ecosystems [*Leroux et al.*, 1995; X.-F. Wen et al., Dew water isotopic ratios and their relations to ecosystem water pools and fluxes in a cropland and a grassland in China, submitted to *Oecologia*, 2010]. Second, variation in flux footprint relative to the location of biomass sampling may introduce discrepancies since soil water and rooting depth can vary significantly at this site [*Welp et al.*, 2008]. Resistivity measurements at this site indicate substantial variation in the upper soil horizon thickness and texture, which has a strong influence on the spatial variation of soil water content. Such heterogeneity could significantly impact the comparison between δ_x and δ_E. Third, long-term eddy covariance data inevitably have missing observations due to equipment malfunction or filtering criteria based on quality control measures. The fact that there are missing flux data from our seasonal time series has potential to bias the comparison.

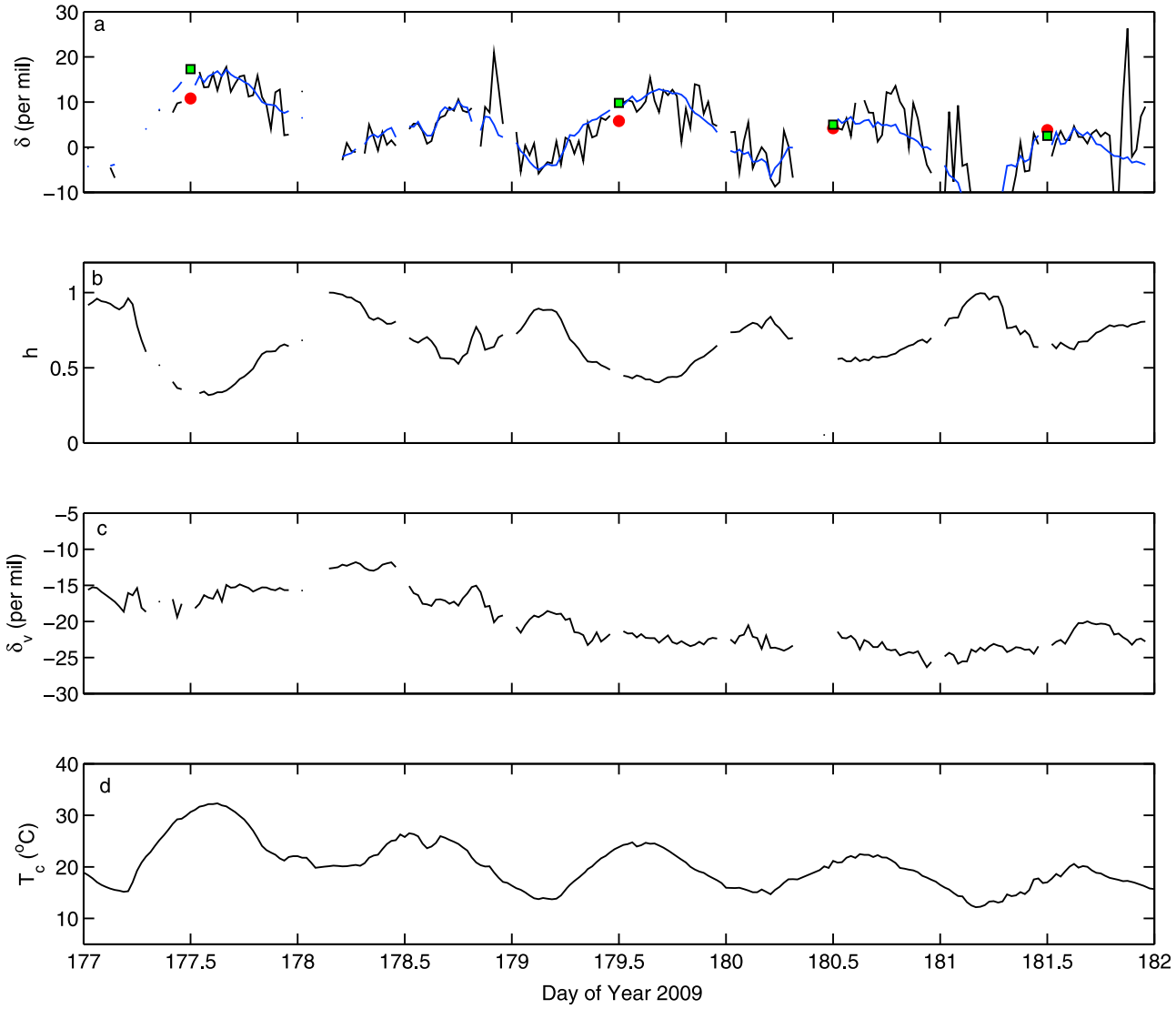

Figure 4. Time series of (a) the isotopic composition at the sites of evaporation determined from steady state (blue line) and non-steady-state (black line) methods. Also shown are the bulk leaf water isotope values extracted from upper (green square) and lower (red circle) canopy leaves; (b) relative humidity determined at the canopy temperature; (c) isotope composition of water vapor; (d) canopy temperature.

[37] *Griffis et al.* [2010b] have shown that δ_E has a pronounced diurnal pattern with relatively strong and progressive enrichment through the day ranging from about −20‰ before sunrise to about −5‰ in late afternoon. Nighttime values were highly variable and depended on the formation of dew. If the data are filtered to remove condensation events, δ_E values were generally more positive at night (up to 30‰). The flux-weighted δ_E values for June, July, and August were −6.8‰, −9.7‰, and −6.1‰, respectively, and differed by 0.4 to 2.7‰ relative to δ_x for June, July, and August. *Welp et al.* [2008] observed δ_E values that were 0.8 to 3.3‰ enriched compared to δ_x based on flux-gradient measurements above a soybean canopy at the same site.

4.4. Temporal Dynamics of Leaf Water Enrichment

[38] A short time series of $\delta_{L,s}$ and $\delta_{L,e}$ is shown in Figure 4 along with the midday values of $\delta_{L,b}$. These data illustrate the dynamic nature of $\delta_{L,e}$ with midday values ranging from about 15‰ on DOY 177 decreasing progressively over the period to about 3‰ on DOY 181. The values of $\delta_{L,b}$ tracked $\delta_{L,e}$ reasonably well, showing a general decrease over the same period. The progressive decrease in $\delta_{L,b}$, $\delta_{L,e}$, and $\delta_{L,s}$ over this period is directly related to the decrease in δ_v and increase in midday relative humidity, which in this case illustrates the strong link to changing meteorological conditions.

[39] During June the mean δ_x was −7.4 ± 1.5‰ and δ_E was −6.8‰. In general, $\delta_{L,e}$ ranged from about −5‰ at 0500 to about 10‰ between 1400 and 1700 LST (Figure 5). The mean midday $\delta_{L,b}$ values for top and bottom leaves were 5.3 and 8.5‰, respectively. The supporting environmental data are also shown in Figure 5. We note that the water vapor canopy conductance ($g_c = 1/r_c$) was slightly positive at night (i.e., a minimum conductance of about 0.05 mol m^{-2} s^{-1}). It was during this time period that the difference between $\delta_{L,s}$ and $\delta_{L,e}$ was relatively large. Notice that the canopy-scale

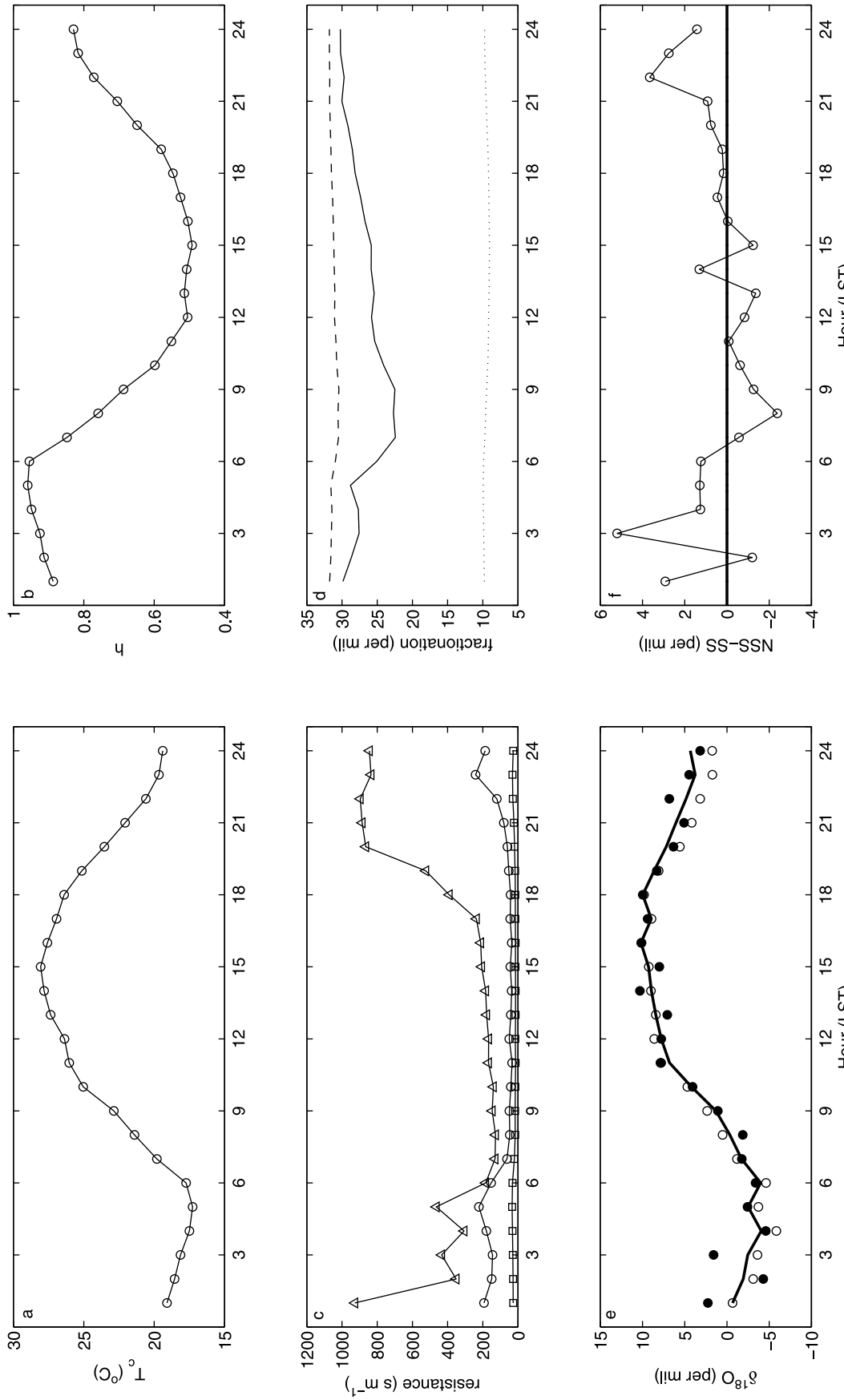

Figure 5. Estimating the oxygen isotope composition at the sites of leaf evaporation. Ensemble patterns are shown for June 2009 corn canopy. (a) Canopy temperature; (b) relative humidity at the leaf surface; (c) resistance values including canopy (triangle), aerodynamic (circle), and boundary layer (square); (d) fractionation factors including equilibrium (dotted line) and kinetic fractionation based on leaf-level formulation (no turbulence, dashed line) and canopy-scale formulation (solid line, with turbulence). (e) Steady state (open circle) versus non-steady-state (solid black circle) values of the oxygen isotope composition at the sites of leaf evaporation. The solid black line indicates the modeled isotope composition at the sites of leaf evaporation based on *Dongmann et al.* [1974]. (f) The difference between the non-steady-state and steady state values.

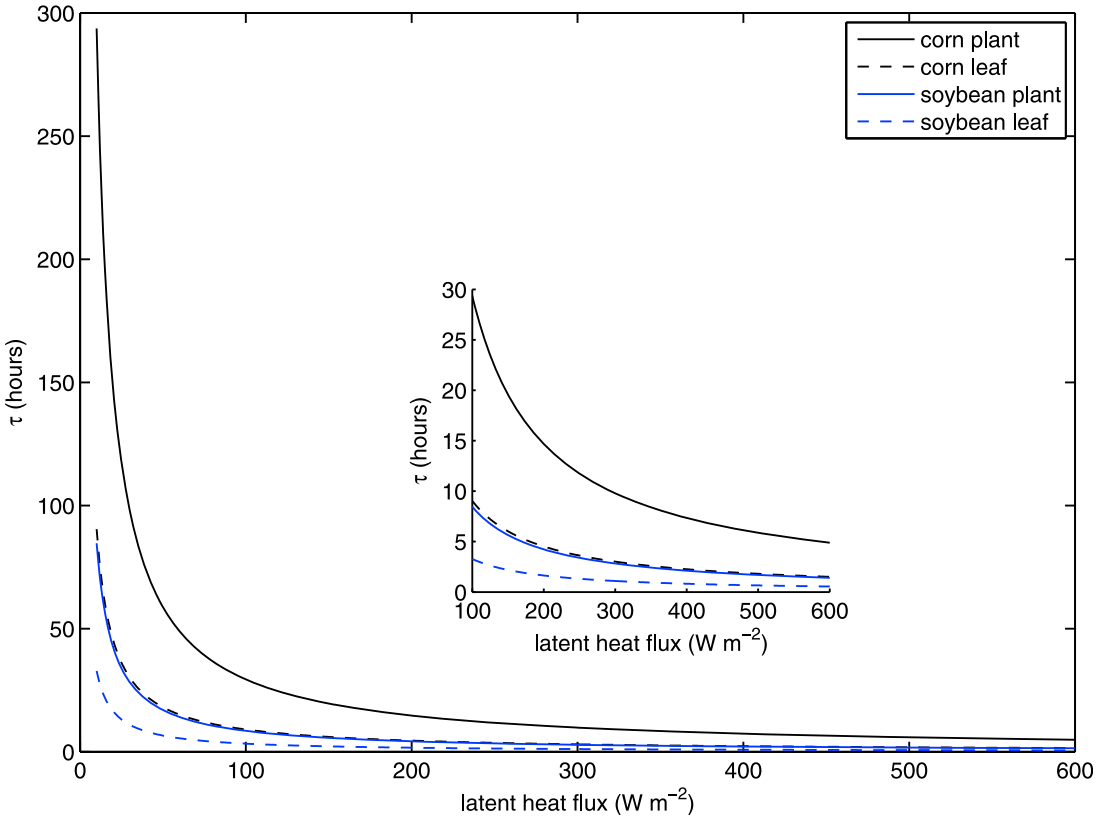

Figure 6. Turnover time of leaf water for soybean and corn as a function of latent heat flux.

kinetic fractionation factor shows a strong diurnal pattern, reaching a minimum of 22.3‰ during early to mid morning as turbulence develops and the canopy becomes more strongly coupled to the atmosphere. The mean kinetic fractionation value for the period was 27.0‰ and was about 4.3‰ lower than the mean leaf value, which does not include the effects of turbulence.

[40] Differences in the diurnal ensemble values of $\delta_{L,s}$ and $\delta_{L,e}$ are also shown in Figure 5. The largest differences, 2 to 5‰, were observed at night with smaller fluctuations observed near midday and late afternoon. A regression analysis using all half-hourly values for the period indicated that $\delta_{L,s}$ was typically 0.6‰ higher than $\delta_{L,e}$. *Welp et al.* [2008] reported soybean $\delta_{L,s}$ values that were typically lower than $\delta_{L,e}$ whereas *Lai et al.* [2006a, 2006b] showed that $\delta_{L,s}$ was significantly more enriched relative to $\delta_{L,e}$ for a Pacific Northwest Douglas-fir forest. These differences can have important implications for predicting the ^{18}O-CO_2 photosynthetic discrimination. Based on these data and analyses we hypothesize that the greater turnover time of leaf water for corn is the primary factor determining the departure from the steady state assumption. Figure 6 illustrates the leaf water turnover (in hours) as a function of latent heat flux, using typical water contents for soybean and corn leaves of 110 and 240 g m^{-2}, respectively. Using the non-steady-state model of *Dongmann et al.* [1974], and the leaf water turnover rate (shown in Figure 6), we show excellent agreement with the $\delta_{L,e}$ values in Figure 5. However, in July and August there appears to be a late afternoon/evening bias that we suspect is related to using a constant leaf water content. Based on field observations of leaf water content in corn at field sites in China, we observed a general dehydration over the course of the day with values becoming relatively stable through the early afternoon. Better observations of absolute leaf water content would help to improve these comparisons. The good agreement observed between the non-steady-state model and field observations at midday also suggests that the contribution of soil evaporation is not significant.

[41] During July (peak growth phase) the differences between $\delta_{L,s}$ and $\delta_{L,e}$ revealed a very pronounced pattern (Figure 7). $\delta_{L,e}$ ranged from about 0‰ at midnight to −4‰ in the early morning. Midday values of $\delta_{L,e}$ peaked at about 10‰ and decreased to about 5‰ after sunset. $\delta_{L,s}$ was consistently higher than $\delta_{L,e}$ from about 0700 to 1200. In general, steady state was only achieved for a few hours after midday, when δ_E values approached −7.1‰. A regression analysis, using all half-hourly data for the period, yielded the following relation, $y = 0.85x + 1.2$($r^2 = 0.76$), indicating that $\delta_{L,s}$ was about 0.7‰ higher than $\delta_{L,e}$. Further, the difference between $\delta_{L,e}$ and $\delta_{L,s}$ appeared to be positively correlated with relative humidity ($y = 4.1h - 3.2$, $r^2 = 0.66$) suggesting that the difference was not a simple artifact of spatial sample variation in δ_x or differences in flux footprint. As expected, the difference between steady state and non-steady-state tended to be large when F_E was small (i.e., as the turnover time of the leaf water increased). The results for August are also shown in Figure 8 and confirm the patterns observed in July. Here, the model results show relatively good agreement at midday, but a relatively strong bias is

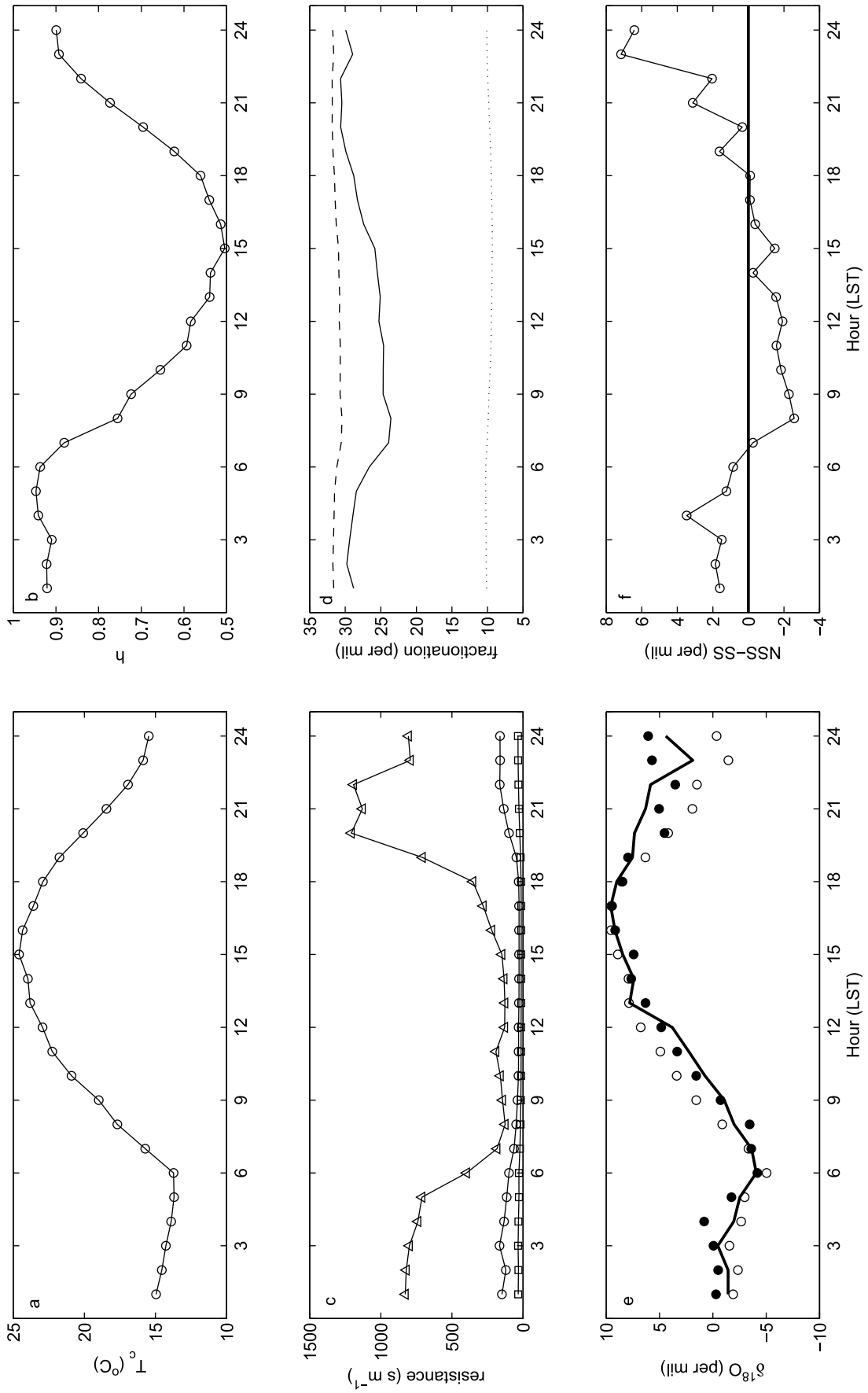

Figure 7. As in Figure 5, except for July 2009.

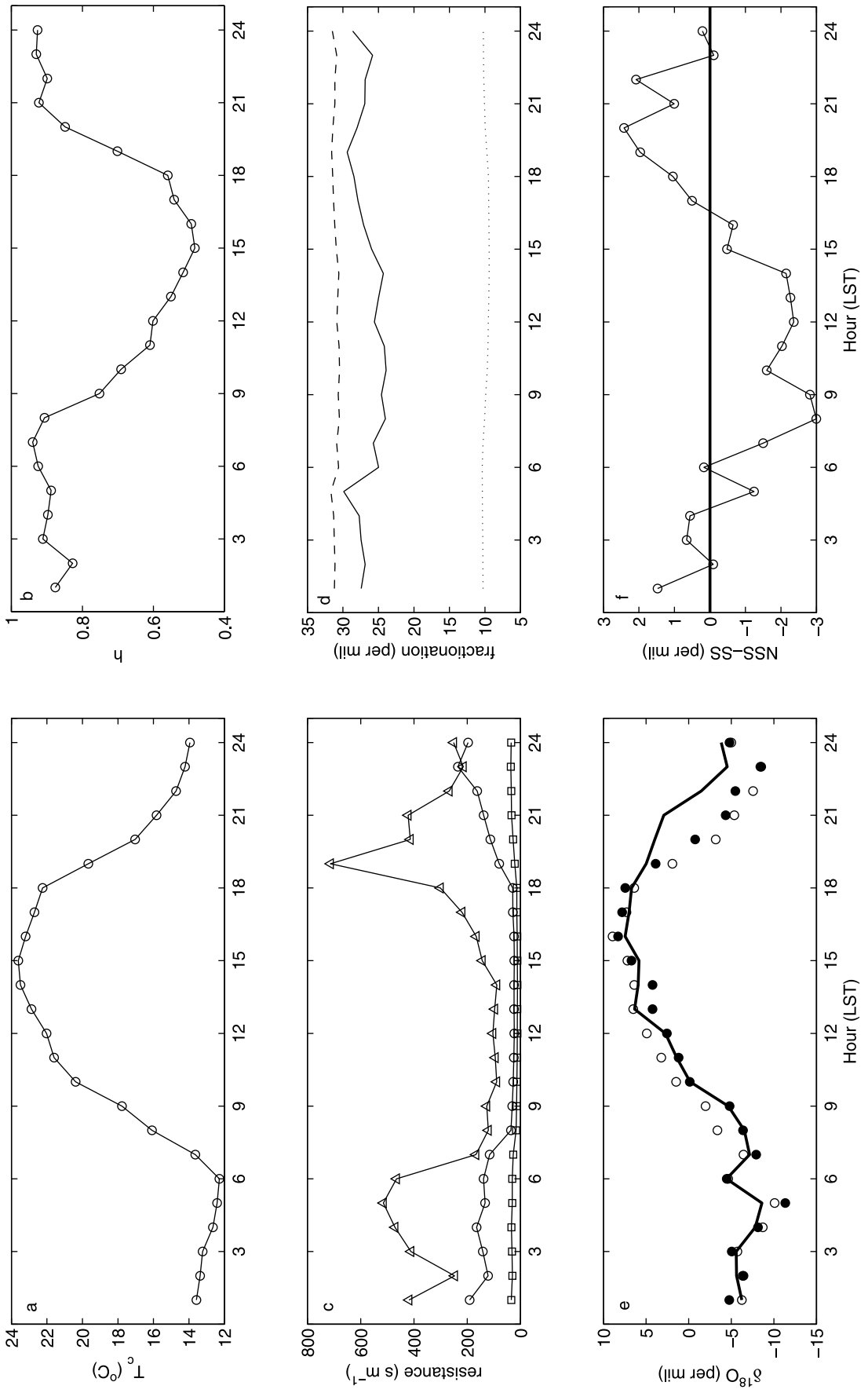

Figure 8. As in Figure 5, except for August 2009.

Table 3. Carbonic Anhydrase Activity and Leaf-Level Oxygen Isotope CO_2 Hydration Efficiency[a]

Leaf Position	CA_{assay} (molar)	CA_{leaf} (molar)	$\theta_{eq,leaf}$
Lower leaf	20.3	43.1	0.79
Base	12.7	25.5	0.65
Mid	29.5	65.3	0.93
Tip	18.7	38.6	0.79
Upper leaf	26.5	76.3	0.62
Base	22.9	60.9	0.56
Mid	31.7	87.2	0.68
Tip	24.8	80.8	0.64

[a]The activity of carbonic anhydrase within the leaf assay (CA_{assay}), corrected for in vivo leaf temperature conditions (CA_{leaf}), and the extent of isotopic equilibrium ($\theta_{eq,leaf}$) between CO_2 and water in plant leaves.

observed during late afternoon and evening. These patterns appear to be consistent with results reported by *Lee et al.* [2007] for a mixed forest in Connecticut and leaf-level laboratory experiments [*Wang and Yakir*, 1995].

4.5. The ^{18}O-CO_2 Discrimination, Extent of ^{18}O Equilibration, and Disequilibrium

[42] The analyses presented above focused on obtaining the key boundary conditions (i.e., $\delta_{L,e}$) for understanding ^{18}O-CO_2 exchange and discrimination. Here we bring together the water and carbon isotope observations to help constrain the extent of ^{18}O-CO_2 equilibration, discrimination, and ^{18}O-CO_2 disequilibrium.

4.5.1. Carbonic Anhydrase Activity

[43] The leaf-scale analysis of *Zea mays* CA activity showed that the CA_{assay} increased from the base (petiole) of the leaf to midleaf and then decreased toward the leaf tip (Table 3). This is consistent with other CA analyses performed on *Zea* mays [*Affek et al.*, 2006]. This trend was also observed in the CA_{leaf} values, where the assay activity was expressed for specific leaf conditions. The CA_{leaf} values were used to calculate the extent of isotope equilibrium between CO_2 and H_2O within the leaf ($\theta_{eq,leaf}$), where the highest values were observed at midleaf.

[44] Our CA activity estimates were similar to other published data on *Zea mays* [*Gillon and Yakir*, 2000b; *Affek et al.*, 2006]. The $\theta_{eq,leaf}$ values estimated here, however, were lower than those observed by *Gillon and Yakir* [2000b] ($\theta_{eq,leaf} \approx 0.8$) and *Affek et al.* [2006] ($\theta_{eq,leaf} \approx 0.9$). Like these previous studies, we found that the equilibrium values for corn were significantly higher than for other C_4 species. Further, $\theta_{eq,leaf}$ is dependent on the estimation of total leaf conductance to CO_2, where higher conductance values resulted in lower $\theta_{eq,leaf}$. For example, calculations of $\theta_{eq,leaf}$ using CO_2 conductance values from mid-August 2009, which were higher than those calculated for the CA leaf sample dates of 31 August and 1 September 2009, caused the average $\theta_{eq,leaf}$ value to decrease slightly from 0.71 to

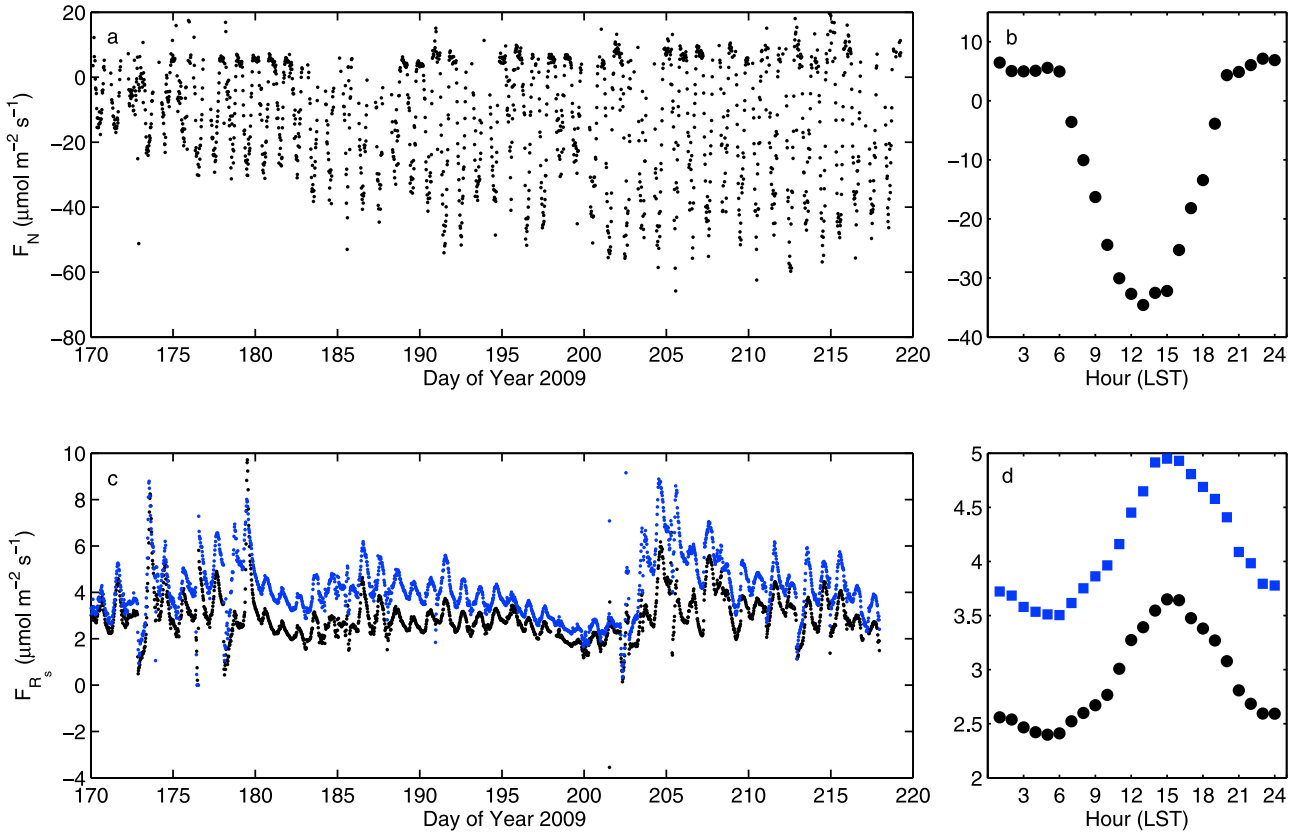

Figure 9. (a) Net ecosystem CO_2 exchange measured with eddy covariance over a C_4 corn canopy during the 2009 growing season; (b) ensemble diurnal pattern of net ecosystem CO_2 exchange; (c) time series of soil respiration measured with two automated soil chambers; (d) ensemble diurnal pattern of soil respiration.

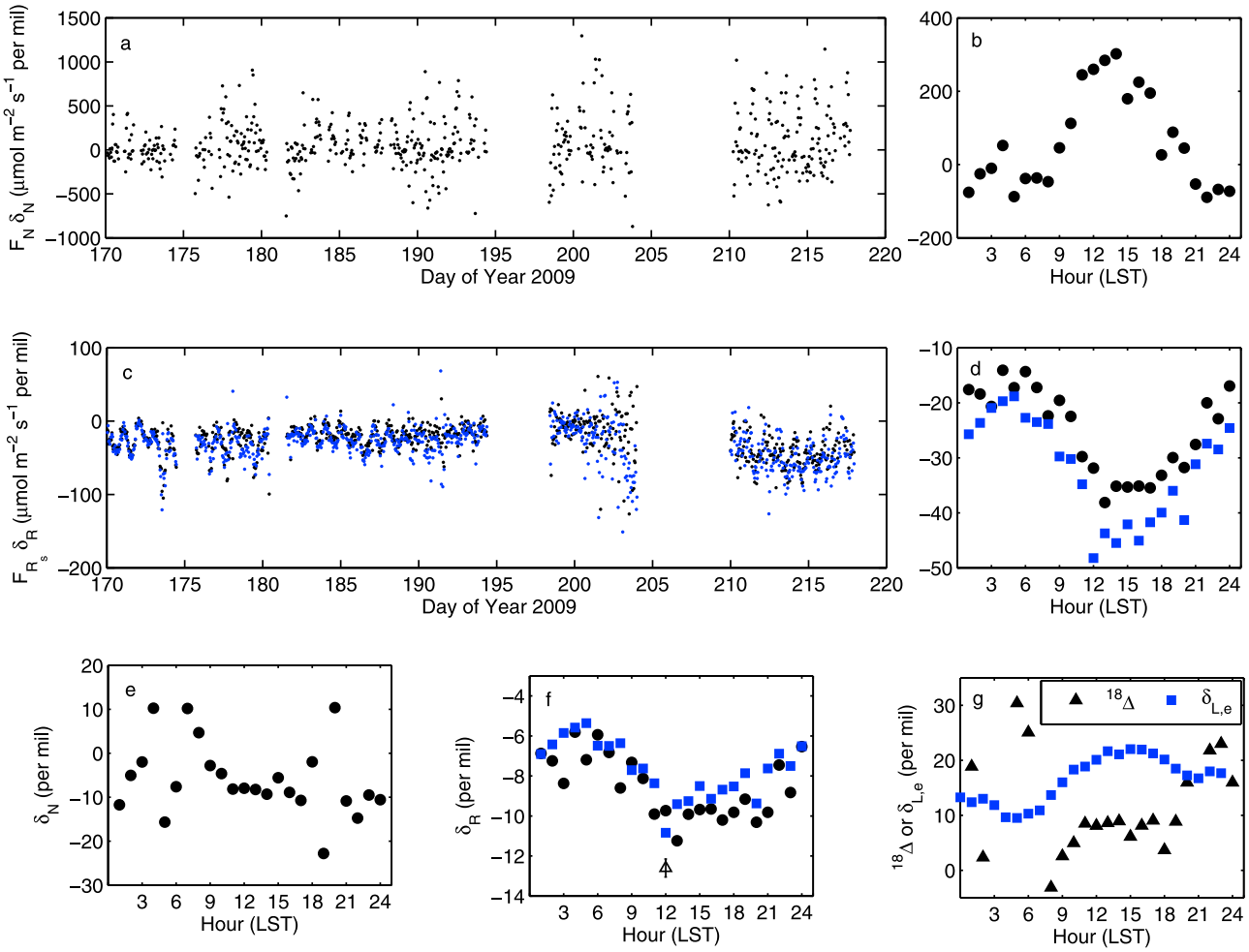

Figure 10. Time series and typical patterns of oxygen isotope CO_2 exchange over a C_4 corn canopy. (a) Net ecosystem CO_2 isoflux measured with a combination of eddy covariance and isotope flux-gradient technique; (b) ensemble diurnal pattern of net ecosystem CO_2 isoflux; (c) soil respiration isoflux measured with an automated soil chamber system coupled to a tunable diode laser; (d) ensemble diurnal pattern of soil CO_2 isoflux; (e) ensemble diurnal pattern of isotope signature of net ecosystem CO_2 exchange; (f) ensemble diurnal pattern of isotope signature of soil respiration; (g) ^{18}O-CO_2 photosynthetic discrimination determined from mass balance and isotope composition at the sites of leaf water evaporation. All variables are expressed on the VPDB scale.

0.66. From these very limited data it appears that $\theta_{eq,leaf}$ is lower for the upper sunlit leaves, which have higher CO_2 conductance values compared to leaves lower in the canopy.

4.5.2. Net Ecosystem CO_2 Exchange and Soil Respiration

[45] Figure 9 reveals the highly productive nature of C_4 corn ecosystems with maximum half-hourly CO_2 uptake reaching 60 μmol m^{-2} s^{-1}. Maximum nighttime half-hourly values (ecosystem respiration) were approximately 20 μmol m^{-2} s^{-1}, indicating that the upper limit of daytime photosynthesis was about 80 μmol m^{-2} s^{-1}. Figure 9 (bottom) illustrates the soil respiration values measured from two automated soil chambers. Soil respiration decreased significantly from DOY 196 to DOY 204 as soil water content decreased to about 0.20 m^3 m^{-3}. The ensemble diurnal patterns derived from both chamber time series indicate that soil respiration reached a mean daytime maximum of about 5 μmol m^{-2} s^{-1} and that the soil respiration represented approximately 35 to 52% of the mean nighttime ecosystem respiration determined from eddy covariance.

[46] The ^{18}O-CO_2 isoflux of net ecosystem exchange and net soil efflux are shown in Figure 10. While these time series reveal considerably more noise than the standard eddy covariance and automated chamber half-hourly values, the ensemble diurnal patterns give important insights regarding the influence of C_4 vegetation on ^{18}O-CO_2 exchange. Typical midday values of F_δ were 300 μmol m^{-2} s^{-1}‰, significantly larger than values measured over C_3 soybean using the eddy covariance and flux-gradient approach [*Griffis et al.*, 2005b, 2008; *Xiao et al.*, 2010] and show similar diurnal variation as model estimates for grasslands [*Still et al.*, 2005]. The relatively large positive values for C_4 vegetation indicate stronger enrichment of the surface layer air in ^{18}O-CO_2, presumably because the large photosyn-

Table 4. Canopy-Scale ^{18}O-CO_2 Discrimination and Isotopic Disequilibrium Assuming Non-Steady-State Conditions[a]

Time Period	LAI (m^2 m^{-2})	h_c (m)	ϵ_k^w (‰)	ϵ_k^c (‰)	$^{18}\Delta$ (‰)	δ_R (‰)	$\delta_{L,e}^c$ (‰)	D_{eq} (‰)	$\frac{C_s}{C_a-C_s}$	F_P (μmol m^{-2} s^{-1})	g_c (mol m^{-2} s^{-1})
Including the Effects of Turbulence[b]											
DOY 170 to 220	3.6	2.2	28.3	8.1	17.0	−9.2	17.1	7.1	0.91	22.7	0.20
DOY 170 to 195	1.6	1.0	27.2	7.9	21.3	−7.0	17.9	12.2	1.29	19.7	0.21
DOY 196 to 220	4.1	2.5	28.5	8.1	12.1	−12.0	16.4	0.7	0.44	27.1	0.19
DOY 170 to 179	1.2	0.8	26.5	7.7	27.5	−8.2	18.7	17.1	1.52	15.6	0.18
DOY 180 to 189	2.0	1.2	26.6	7.7	20.3	−6.7	15.4	12.3	1.28	18.4	0.22
DOY 190 to 199	3.6	2.1	29.0	8.2	16.1	−5.6	18.5	7.8	0.90	25.3	0.18
DOY 200 to 209	3.6	2.4	27.3	7.9	13.1	−12.1	16.5	0.3	0.56	24.9	0.22
DOY 210 to 219	5.2	2.6	27.5	7.9	11.3	−13.1	16.1	0.6	0.32	28.1	0.19
Not Including the Effects of Turbulence											
DOY 170 to 220	3.6	2.2	31.5	8.7	19.7	−9.2	18.7	9.0	0.91	22.7	0.20
DOY 170 to 195	1.6	1.0	31.3	8.6	25.0	−7.0	19.5	15.4	1.29	19.7	0.21
DOY 196 to 220	4.1	2.5	31.5	8.7	13.7	−12.0	18.8	2.7	0.44	27.1	0.19
DOY 170 to 179	1.2	0.8	31.2	8.6	31.4	−8.2	20.4	20.5	1.52	15.6	0.18
DOY 180 to 189	2.0	1.2	31.2	8.6	24.1	−6.7	17.4	16.0	1.28	18.4	0.22
DOY 190 to 199	3.6	2.1	31.6	8.7	18.2	−5.6	19.8	9.4	0.90	25.3	0.18
DOY 200 to 209	3.6	2.4	31.3	8.6	15.3	−12.1	18.1	3.2	0.56	24.9	0.22
DOY 210 to 219	5.2	2.6	31.2	8.6	12.6	−13.1	18.8	1.8	0.32	28.1	0.19

[a]Here we have used a value of 0.71 for θ_{eq}. D_{eq} is the isotope disequilibrium (absolute value) and represents the difference between the isotope composition of photosynthesis and net soil efflux. All values represent the median values during the daytime (0500–2000 LST).
[b]The analyses includes the influence of turbulence on the kinetic fraction calculations of water vapor and carbon dioxide.

thetic flux counteracts the lower CO_2 hydration efficiency that is associated with C_4 corn.

[47] The seasonal variation in the net soil isoflux revealed a trend that was consistent with the variation in the isotope composition of soil water (see Figures 3b and 10c). Net soil isoflux values at midday were about −50 μmol m^{-2} s^{-1}‰, partially counteracting the influence of the C_4 photosynthetic isoflux. These chamber data indicate that the isotope composition of midday net soil efflux ranged between −14‰ and −12‰ over the course of the measurement period. In general, these values are similar to midsummer soil respiration observations from southern boreal forests [*Flanagan et al.*, 1997], a temperate forest near Borden, Ontario (E. Santos et al., Temporal dynamics of $^{13}CO_2$ and $C^{18}O^{16}O$ near the ground and above a temperate deciduous forest, manuscript in preparation, 2011), but are significantly more depleted compared to soil chamber observations from a recent study in southern Portugal [*Wingate et al.*, 2008] owing to the large differences in the isotope composition of the soil water in these very different climates. Global estimates of the isotope composition of the net soil efflux are on the order of −7.9‰ [*Yakir*, 2003].

[48] Since the invasion of atmospheric ^{18}O-CO_2 into the soil profile can influence the isotope composition of soil respiration [*Tans*, 1998], we also estimated the expected isotope composition of soil respiration assuming full isotope equilibration with the soil water measured at a depth of 10 cm (Figure 10f). From these data we estimated a mean value and standard error of −13.2 ± 0.45‰ (i.e., $\delta_R = \delta_s^c - \epsilon_k^c =$ −4.5‰ − 8.7‰). This value is within the range of that observed from the chambers suggesting that the chamber measurements provided a reasonable constraint on the soil CO_2 isoflux. The disparity may be attributed to a soil CO_2 signal that is influenced by the isotope ratio of the soil water at a deeper depth, soil CO_2 that equilibrated with the soil water closer to the surface (i.e., upper 10 cm), non-steady-state impacts on the chamber measurement [*Nickerson and Risk*, 2009; *Powers et al.*, 2010], or the influence of carbonic anhydrase activity in the soil. From the theory presented by *Wingate et al.* [2009, 2010] we also calculated the soil carbonic anhydrase enhancement factor (f_{CA}) and the soil depth where full equilibration between water and soil CO_2 occurs (z_{eq}). We estimated an f_{CA} value of 20 with z_{eq} located at approximately 2 cm. Our estimate of f_{CA} suggests that CA activity is present, but is at the lowest end of the range (20 to 300) reported by *Wingate et al.* [2009].

4.5.3. Temporal Variability in $^{18}\Delta$ and Disequilibrium

[49] We used the ensemble patterns of the data shown in Figures 9 and 10 to constrain $^{18}\Delta$ based on a mass balance approach (equation (6)). We observed midday $^{18}\Delta$ values of approximately 9‰ with large variations during early morning and at night when the fluxes of water and carbon tended to be small (Figure 10g). These midday ^{18}O-CO_2 discrimination values were significantly lower than those reported for our soybean experiments [*Griffis et al.*, 2005b; *Xiao et al.*, 2010].

[50] In a second approach we used equation (4) and our estimate of $\theta_{eq,leaf}$ to calculate $^{18}\Delta$ for a range of phenological windows (Table 4). Over the main measurement period (DOY 170 to DOY 220) the median daytime (0500–2000 LST) $^{18}\Delta$ was 17.0‰. The maximum value (27.5‰) was observed in mid June (DOY 170 to DOY 179) and decreased steadily to 11.3‰ by the end of the main measurement period (August). In general, these estimates were significantly higher (nearly double) than those obtained from the mass balance approach described above.

[51] Table 4 presents the ^{18}O-CO_2 disequilibrium (absolute values, with $^{18}\Delta$ derived from equation (4)), which ranged from 0.3 to 17.1‰ over the duration of the study period. The median daytime value was 7.8‰. In comparison to ^{13}C-CO_2 measurements over a corn canopy at the same site, isotope disequilibrium was typically larger for the ^{18}O-CO_2 tracer. As described previously, ^{13}C-CO_2 disequilibrium of C_4 corn rapidly diminishes through the growing season as

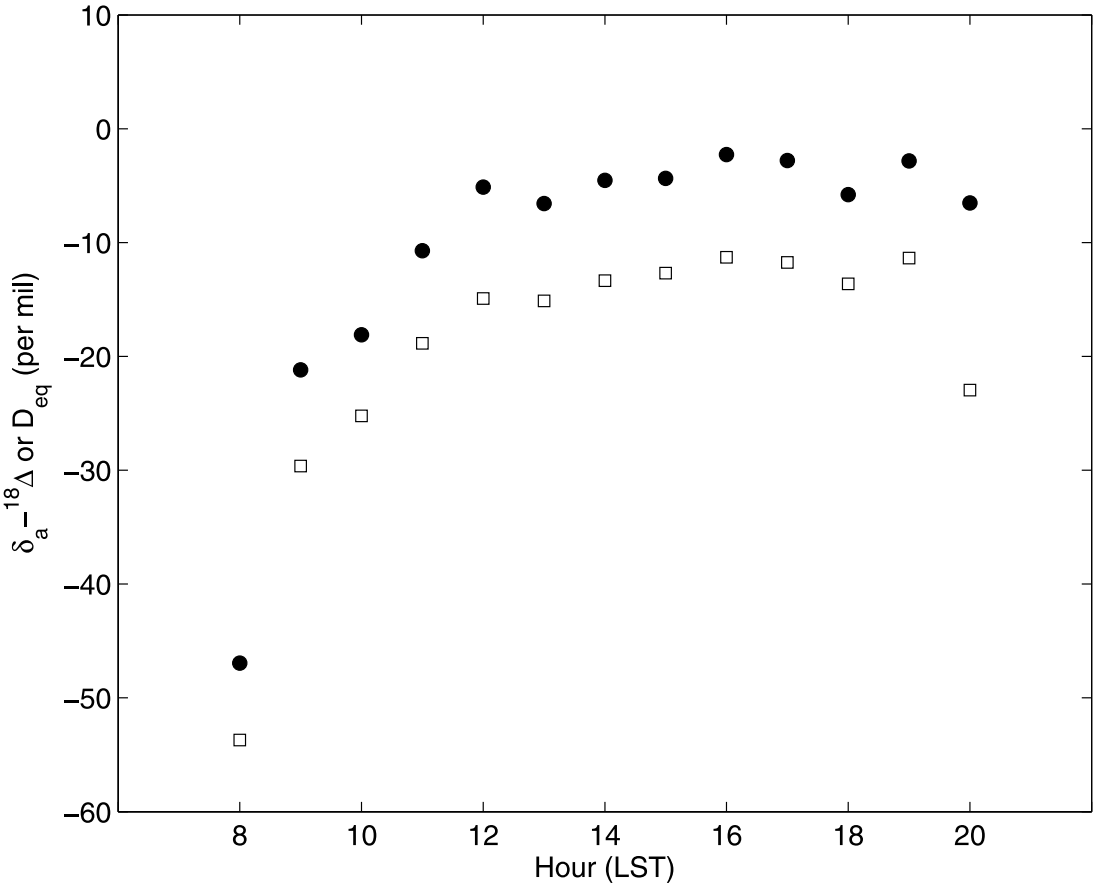

Figure 11. Diurnal ensemble of the modeled oxygen isotope composition of photosynthesis (open square) and corresponding oxygen isotope disequilibrium value (solid circle). Here the disequilibrium values are calculated as $D_{eq} = \delta_R - (\delta_a - {}^{18}\Delta)$.

Table 5. Canopy-Scale ^{18}O-CO_2 Discrimination and Isotopic Disequilibrium Assuming Steady State Conditions[a]

Time Period	LAI (m^2 m^{-2})	h_c (m)	ϵ_k^w (‰)	ϵ_k^c (‰)	$^{18}\Delta$ (‰)	δ_R (‰)	$\delta_{L,e}^c$ (‰)	D_{eq} (‰)	$\frac{C_s}{C_a - C_s}$	F_P (μmol m^{-2} s^{-1})	g_c (mol m^{-2} s^{-1})
Including the Effects of Turbulence[b]											
DOY 170 to 220	3.6	2.2	28.3	8.1	19.1	−9.2	19.3	8.2	0.91	22.7	0.20
DOY 170 to 195	1.6	1.0	27.2	7.9	23.6	−7.0	18.8	14.0	1.29	19.7	0.21
DOY 196 to 220	4.1	2.5	28.5	8.1	13.6	−12.0	19.7	2.6	0.44	27.1	0.19
DOY 170 to 179	1.2	0.8	26.5	7.7	26.6	−8.2	18.2	17.6	1.52	15.6	0.18
DOY 180 to 189	2.0	1.2	26.6	7.7	22.6	−6.7	18.0	14.5	1.28	18.4	0.22
DOY 190 to 199	3.6	2.1	29.0	8.2	19.3	−5.6	21.2	10.4	0.90	25.3	0.18
DOY 200 to 209	3.6	2.4	27.3	7.9	13.8	−12.1	20.2	0.67	0.56	24.9	0.22
DOY 210 to 219	5.2	2.6	27.5	7.9	12.3	−13.1	19.1	1.41	0.32	28.1	0.19
Not Including the Effects of Turbulence											
DOY 170 to 220	3.6	2.2	31.5	8.7	21.5	−9.2	21.5	9.7	0.91	22.7	0.20
DOY 170 to 195	1.6	1.0	31.3	8.6	27.3	−7.0	21.4	17.7	1.29	19.7	0.21
DOY 196 to 220	4.1	2.5	31.5	8.7	15.2	−12.0	21.5	4.3	0.44	27.1	0.19
DOY 170 to 179	1.2	0.8	31.2	8.6	30.5	−8.2	20.9	21.5	1.52	15.6	0.18
DOY 180 to 189	2.0	1.2	31.2	8.6	26.4	−6.7	20.4	18.3	1.28	18.4	0.22
DOY 190 to 199	3.6	2.1	31.6	8.7	20.6	−5.6	23.0	11.2	0.90	25.3	0.18
DOY 200 to 209	3.6	2.4	31.3	8.6	15.9	−12.1	22.4	2.3	0.56	24.9	0.22
DOY 210 to 219	5.2	2.6	31.2	8.6	13.6	−13.1	21.3	2.6	0.32	28.1	0.19

[a]Here we have used a value of 0.71 for θ_{eq}. D_{eq} is the isotope disequilibrium (absolute value) and represents the difference between the isotope composition of photosynthesis and net soil efflux. All values represent the median values during the daytime (0500–2000 LST).
[b]The analyses includes the influence of turbulence on the kinetic fraction calculations of water vapor and carbon dioxide.

Table 6. Sensitivity Analysis of Canopy-Scale ^{18}O-CO_2 Discrimination and Isotope Disequilibrium[a]

Parameter	$^{18}\Delta$ (‰)	D_{eq} (‰)
$F_P \pm 10\%$	15.1, 19.4 (−1.9, +2.4)	−6.2, −10.5 (+0.9, −3.4)
$C_a \pm 10\%$	19.2, 14.9 (+2.2, −2.1)	−10.2, −6.0 (−3.1, +1.1)
$C_s \pm 10\%$	14.9, 15.3 (−2.1, −1.7)	−5.4, −6.3 (+1.7, +0.8)
$U \pm 10\%$	17.1, 17.4 (+0.1, +0.4)	−8.1, −7.9 (−1.0, −0.8)
$h \pm 10\%$	15.7, 18.4 (−1.3, +1.4)	−6.9, −9.3 (+0.21, −2.2)
$\theta_{eq} \pm 10\%$	18.4, 15.7 (+1.4, −1.3)	−9.4, −6.8 (−2.3, +0.3)
$\delta^c_{L,e} \pm 2‰$	18.4, 15.7 (+1.4, −1.3)	−9.4, −6.8 (−2.3, +0.3)
$\delta_v \pm 2‰$	17.8, 16.4 (+0.8, −0.6)	−8.8, −7.4 (−1.7, −0.3)
$\delta_a \pm 2‰$	15.7, 18.4 (−1.3, +1.4)	−4.8, −11.4 (+2.3, −4.3)

[a]Note that the sensitivity analysis was applied to the period DOY 170 to DOY 220 of Table 4 (including the effects of turbulence). Results are presented for the positive followed by the negative perturbations from the nominal values. Values in parentheses represent the ‰ departure from the nominal values.

the isotope composition of soil respiration equilibrates with recently fixed CO_2 [*Griffis et al.*, 2005a]. The periods of low ^{18}O-CO_2 disequilibrium were correlated with increased precipitation. For instance, the three periods with D_{eq} values approaching 0‰ had precipitation totals greater than 19 mm. The seasonal D_{eq} values measured here are similar to that reported by *Wingate et al.* [2010] and Santos et al. (manuscript in preparation, 2011). Figure 11 illustrates the daytime ensemble pattern of D_{eq} for the growing season and indicates a very dynamic range (45 to 2‰) with a strong reduction toward late afternoon. It should be noted that the D_{eq} values based on the mass balance approach were considerably lower (≈2‰).

[52] The analyses presented in Tables 4 and 5 confirm that the typical daytime steady state ($\delta_{L,s}$) values were about 2.2‰ higher than the non-steady-state ($\delta_{L,e}$) estimate. This corresponded with a 2.1‰ higher $^{18}\Delta$ value for steady state conditions and a 1.1‰ higher disequilibrium value. It is also interesting to note that ignoring the influence of turbulence on kinetic fractionation also caused the isotope disequilibrium to be larger (i.e., accounting for the influence of turbulence on kinetic fractionation acted to diminish the calculated isotope disequilibrium).

[53] A number of interacting environmental factors determine $^{18}\Delta$. Table 6 presents a sensitivity analysis to help understand its variability. As expected, the factors with the highest sensitivity were F_P, C_c, and C_a since they directly impact the magnitude of the retroflux (i.e., $C_c/(C_a - C_c)$). It is also important to note the number of indirect factors that have relatively high sensitivity. Of particular interest, h and δ_v have an important influence on the boundary condition $\delta_{L,e}(\delta^c_{L,e})$. Typical diurnal patterns of δ_v at this site indicate that it is relatively more depleted during midday than at night. For instance, during the mid growing season it ranged from about −18‰ at night to about −20‰ before midday [*Griffis et al.*, 2010b]. Similar patterns have been reported by *Lee et al.* [2006], *Welp et al.* [2008], and *Lai et al.* [2006a, 2006b], which provide indirect evidence of the strong influence of water vapor entrainment from above the planetary boundary layer (PBL).

[54] Direct observations of the entrainment flux or isotope composition of the entrainment layer air are exceptionally rare. *He and Smith* [1999] observed δ_v values < −40‰ above the PBL based on aircraft flask measurements. *Lee et al.* [2006] used those values to estimate an entrainment flux ratio of −20.7‰. The entrainment water vapor flux has been shown to be approximately 1.6 times the surface water vapor flux [*Barr and Betts*, 1997; *Davis et al.*, 1997], having an overall net drying effect on the PBL. A back-of-the-envelope calculation, therefore, suggests that the entrainment isoflux is about 330 mmol m^{-2} s^{-1}‰. Thus, entrainment can play a dominant role in determining the isotope composition of the surface layer and represents an important PBL feedback effect on influencing the isotope composition of the leaf water and, indirectly, ^{18}O-CO_2 photosynthetic discrimination. Strong entrainment will have two opposing effects on the isotope composition of leaf water. It will cause δ_v to be relatively more depleted, but it will also reduce the surface layer relative humidity, thereby, enhancing kinetic fractionation. The development of clouds in the convective boundary layer can also influence h and δ_v. Further, clouds can have an important impact on ^{18}O-CO_2 flux because of their influence on the amount and quality of diffuse radiation absorbed by a canopy [*Still et al.*, 2009].

[55] Table 6 also highlights that $^{18}\Delta$ has a strong sensitivity to the CO_2 hydration efficiency, which cannot be measured directly at the canopy scale. *Xiao et al.* [2010] used a combination of measurements and modeling to optimize the canopy-scale CO_2 hydration efficiency of a C_3 soybean canopy. They demonstrated that θ_{eq} was about 0.46, or roughly half the value that has been observed in laboratory conditions or prescribed in global isotope tracer models. If we optimize θ_{eq} based on our isoflux measurements and numerical approach we too estimate θ_{eq} that is considerably lower ($\theta_{eq} = 0.196 \pm 0.08$) than our leaf-level observations or the previously reported values in the literature. This is consistent with our relatively lower estimate of $^{18}\Delta$ based on the mass balance approach.

[56] There are a number of potential explanations for this observed discrepancy in $^{18}\Delta$. First, an underestimate of the ^{18}O-CO_2 isoflux at the canopy scale would cause the mass balance estimate of $^{18}\Delta$ to be underestimated. In 2006, we measured the ^{18}O-CO_2 isoflux at our research site using two different methods including flux gradient and eddy covariance using separate laser systems. We did not observe any appreciable bias between these approaches. In order to account for the above discrepancy we would need to approximately double the ^{18}O-CO_2 isoflux.

[57] Second, it is possible that the net soil isoflux, based on the automated chamber approach, was underestimated. From mass balance, this too would result in an underestimate of $^{18}\Delta$. The chamber soil respiration data appear to be in good agreement relative to the nighttime eddy flux data. The isotope composition of the soil efflux, however, could be an issue since it is relatively more difficult to measure. In order to force better agreement with the model estimate of $^{18}\Delta$, the net soil isoflux would need to be doubled. Assuming the chamber respiration values are correct, then the isotope composition of the soil CO_2 efflux would need to be on the order of −76‰. This seems physically unreasonable based on our soil water isotope analyses. Further, typical soil oxygen isotope ratios reported in the literature generally range from −30 to −5‰ (VPDB-CO_2 scale) including sites from sub tropical forest; Mediterranean evergreen forests; semiarid grasslands; coastal forests; and

boreal forests [*Wingate et al.*, 2008; *Ogée et al.*, 2004; *Lai et al.*, 2006a, 2006b; *Bowling et al.*, 2003b; *Flanagan et al.*, 1999].

[58] Third, the retroflux ($C_s/(C_s - C_a)$) is a key model input. Estimates at the canopy scale indicate that relatively good agreement is observed between the mass balance method and the model approach when the retroflux is less than 0.5. Based on the canopy-scale data we often observed retroflux values that were greater than 0.9 (with a maximum value of 1.5), which are associated with larger values of modeled $^{18}\Delta$. Leaf-level photosynthesis data (samples included top canopy leaf only) collected from the same field site in 2009 indicate that the median value of C_s/C_a was 0.72 and that the median retroflux value was 2.6 ± 2.7. Examination of g_c from leaf-level observations indicate a median value of 0.05 mol m^{-2} s^{-1}. When scaled to the canopy, the values agree closely with the canopy-scale observations. These lines of evidence lead us to believe that the retroflux estimate from the canopy-scale observations are reasonable and not the underlying cause for the disagreement between the mass balance and modeled $^{18}\Delta$.

[59] Finally, the big leaf modeled value of $^{18}\Delta$ may be biased by using a mix of parameters estimated from the canopy and leaf scale. The big leaf estimate of $^{18}\Delta$ is most sensitive to F_P, C_a, C_s, and θ_{eq}. Of these parameters, θ_{eq} was derived from leaf measurements under field conditions, but due to limited data and process understanding, they were not scaled to the canopy in a meaningful way. *Xiao et al.* [2010] reported a similar finding for a soybean canopy at the same research site, but using a very detailed model analysis. In their final assessment, they hypothesized that a lower θ_{eq} under field conditions was the most likely reason for the lower estimate of canopy-scale $^{18}\Delta$. Here, we arrive at a similar conclusion, but for a different photosynthetic pathway (C_4), based on a different methodological approach, and for a different growing season.

[60] At this point it is not clear if there is a real biophysical mechanism that can explain such a large disparity. Leaf-level experiments on a variety of C_4 grasses by *Cousins et al.* [2008] suggest that CA activity could not be used to reliably predict the extent of ^{18}O equilibration between leaf H_2O and CO_2 because CA is not isolated to the sites of CO_2-H_2O exchange. As discussed by *Yakir* [2003], overestimating the CO_2 hydration efficiency will lead to a significant underestimate of the gross ecosystem photosynthesis based on inverse analyses. A θ_{eq} value of 0.20 implies that only 20% of the photosynthetic CO_2 retroflux equilibrated with $\delta_{L,e}$ and that there is relatively weak coupling at the sites of leaf evaporation. It is only within the last few years that we have developed the capacity to investigate such questions under field conditions and at the canopy scale. Continued research and improvement in the measurement techniques should help to resolve these key questions.

5. Conclusions

[61] 1. Based on eddy covariance water vapor isotope flux measurements we estimated the oxygen isotope composition at the sites of leaf water evaporation for a C_4 (corn) canopy. We observed diurnal patterns of leaf water ^{18}O enrichment that were very similar to those of previous measurements over a C_3 soybean canopy. However, there were important differences that emerged from the steady state versus non-steady-state calculations. The steady state assumption resulted in values that were up to 3‰ higher than non-steady-state calculations during the daytime for the C_4 canopy. This difference has important implications for estimating the ^{18}O-CO_2 isoflux, photosynthetic discrimination, and disequilibrium. In general, the ^{18}O-CO_2 isoflux was larger for corn than soybean, but this was attributed to a large photosynthetic flux that countered the weaker photosynthetic discrimination.

[62] 2. From simultaneous measurements of ^{18}O-CO_2 and ^{18}O-H_2 O isofluxes, we have provided constraints on the canopy-scale CO_2 hydration efficiency. In this study, the mean optimized value for the growing season was 0.196 ± 0.08 and was significantly lower than leaf-level values of about 0.70. This suggests that ^{18}O coupling between CO_2 and H_2O within C_4 (corn) leaves is relatively weak at the canopy scale. There is growing evidence in the scientific literature that the CO_2 hydration efficiency is significantly lower than observed under laboratory conditions for both C_3 and C_4 ecosystems.

[63] 3. We observed significant seasonal variation in the modeled ^{18}O-CO_2 isotope disequilibrium. In general, the disequilibrium was relatively large (7‰), but there were periods when it diminished to near zero values, which correlated with increased precipitation. The diurnal cycle of isotope disequilibrium was also pronounced, ranging from about 45‰ during the morning to 2‰ during the late afternoon. The calculation of leaf water enrichment based on the steady state assumption resulted in higher ^{18}O-CO_2 photosynthetic discrimination and isotope disequilibrium. Further, explicitly accounting for canopy-scale kinetic fractionation diminished the magnitude of the calculated isotope disequilibrium. The isotope disequilibrium values derived from a mass balance approach were considerably smaller (≈2‰).

[64] **Acknowledgments.** We thank Jeremy Smith and Bill Breiter for their technical assistance in the lab and at the field site. Funding for this research has been provided by the National Science Foundation, ATM-0546476 (T.G.), ATM-0914473 (X.L.),DEB-0514908 (X.L. and T.G.), the Office of Science (BER) U.S. Department of Energy, DE-FG02-06ER64316 (T.G. and J.B.), and the College of Food, Agricultural, and Natural Resource Sciences at the University of Minnesota.

References

Affek, H., M. Krisch, and D. Yakir (2006), Effects of interaleaf variations in carbonic anhydrase activity and gas exchange on leaf $C^{18}OO$ isoflux in zea mays, *New Phytol.*, *169*, 321–329.

Baker, J. M., and T. J. Griffis (2005), Examining strategies to improve the carbon balance of corn/soybean agriculture using eddy covariance and mass balance techniques, *Agric. For. Meteorol.*, *128*, 163–177.

Barr, A., and A. Betts (1997), Radiosonde boundary layer budgets above a boreal forest, *J. Geophys. Res.*, *102*, 29,205–29,212.

Bowling, D. R., S. Sargent, B. Tanner, and J. R. Ehleringer (2003a), Tunable diode laser absorption spectroscopy for stable isotope studies of ecosystem-atmosphere CO_2 exchange, *Agric. For. Meteorol.*, *118*, 1–19.

Bowling, D. R., N. G. McDowell, J. M. Welker, B. J. Bond, B. E. Law, and J. R. Ehleringer (2003b), Oxygen isotope content of CO_2 in nocturnal ecosystem respiration: 2. Short-term dynamics of foliar and soil component fluxes in an old-growth ponderosa pine forest, *Global Biogeochem. Cycles*, *17*(4), 1124, doi:10.1029/2003GB002082.

Brenninkmeijer, C., P. Kraft, and W. G. Mook (1983), Oxygen isotope fractionaton between CO_2 and H_2O, *Isotope Geosci.*, *1*, 181–190.

Cousins, A., M. Badger, and S. von Caemmerer (2008), C_4 photosynthetic isotope exchange in nad-me- and nadp-me-type grasses, *J. Exp. Bot.*, *59*, 1695–1703.

Craig, H., and L. Gordon (1965), Deuterium and oxygen-18 variations in the ocean and the marine atmosphere, in *Proceedings of a Conference on Stable Isotopes in Oceanographic Studies and Paleotemperatures, Spoleto, Italy*, edited by E. Tongiorgi, pp. 9–130, Lab. Geol. Nucl., Pisa, Italy.

Cuntz, M., P. Ciais, G. Hoffmann, C. E. Allison, R. J. Francey, W. Knorr, P. P. Tans, J. W. C. White, and I. Levin (2003a), A comprehensive global three-dimensional model of $\delta^{18}O$ in atmospheric CO_2: 2. Mapping the atmospheric signal, *J. Geophys. Res.*, *108*(D17), 4528, doi:10.1029/2002JD003154.

Cuntz, M., P. Ciais, G. Hoffmann, and W. Knorr (2003b), A comprehensive global three-dimensional model of $\delta^{18}O$ in atmospheric CO_2: 1. Validation of surface processes, *J. Geophys. Res.*, *108*(D17), 4527, doi:10.1029/2002JD003153.

Davis, K. J., D. H. Lenschow, S. P. Oncley, C. Kiemle, G. Ehret, A. Giez, and J. Mann (1997), Role of entrainment in surface-atmosphere interactions over the boreal forest, *J. Geophys. Res.*, *102*(D24), 29,219–29,230.

Dongmann, G., H. Nurnberg, H. Forstel, and K. Wagener (1974), Enrichment of H218O in leaves of transpiring plants, *Radiat. Environ. Biophys.*, *11*, 41–52.

Farquhar, G., and L. Cernusak (2005), On the isotopic composition of leaf water in the non-steady state, *Funct. Plant Biol.*, *32*(4), 293–303, doi:10.1071/FP04232.

Farquhar, G., and J. Lloyd (1993), Carbon and oxygen isotope effects in the exchange of carbon dioxide between terrestrial plants and the atmosphere, in *Stable Isotopes In Plant Carbon-Water Relations*, pp. 47–70, Academic, San Diego, Calif.

Farquhar, G. D., J. Lloyd, J. A. Taylor, L. B. Flanagan, J. P. Syvertsen, K. T. Hubick, S. C. Wong, and J. R. Ehleringer (1993), Vegetation effects on the isotope composition of oxygen in atmospheric CO_2, *Nature*, *363*, 439–443.

Fassbinder, J. J. (2010), Tracing the flow of carbon through ecosystems using stable isotope techniques, Master's thesis, Univ. of Minn., St. Paul.

Flanagan, L. B., J. R. Brooks, G. T. Varney, and J. R. Ehleringer (1997), Discrimination against $C^{18}O^{16}O$ during photosynthesis and the oxygen isotope ratio of respired CO_2 in boreal forest ecosystems, *Global Biogeochem. Cycles*, *11*(1), 83–98.

Flanagan, L. B., D. S. Kubien, and J. R. Ehleringer (1999), Spatial and temporal variation in the carbon and oxygen stable isotope ratio of respired CO_2 in a boreal forest ecosystem, *Tellus, Ser. B*, *51*(2), 367–384.

Gaumont-Guay, D., T. Black, T. Griffis, A. Barr, R. S. Jassal, and Z. Nesic (2006), Interpreting the dependence of soil respiration on soil temperature and water content in a boreal aspen stand, *Agric. For. Meteorol.*, *140*, 220–235.

Gillon, J., and D. Yakir (2001), Influence of carbonic anhydrase activity in terrestrial vegetation on the ^{18}O content of atmospheric CO_2, *Science*, *291*(5513), 2584–2587.

Gillon, J. S., and D. Yakir (2000a), Naturally low carbonic anhydrase activity in C_4 and C_3 plants limits discrimination against $C^{18}OO$ during photosynthesis, *Plant Cell Environ.*, *23*(9), 903–915, 48.

Gillon, J. S., and D. Yakir (2000b), Internal conductance to CO_2 diffusion and (COO)-O-18 discrimination in C_3 leaves, *Plant Physiol.*, *123*(1), 201–213, 43.

Griffis, T. J., T. A. Black, D. Gaumont-Guay, G. B. Drewitt, Z. Nesic, A. G. Barr, K. Morgenstern, and N. Kljun (2004), Seasonal variation and partitioning of ecosystem respiration in a southern boreal aspen forest, *Agric. For. Meteorol.*, *125*(3–4), 207–223.

Griffis, T. J., J. M. Baker, and J. Zhang (2005a), Seasonal dynamics and partitioning of isotopic CO_2 exchange in C_3/C_4 managed ecosystem, *Agric. For. Meteorol.*, *132*(1–2), 1–19.

Griffis, T. J., X. Lee, J. M. Baker, S. D. Sargent, and J. Y. King (2005b), Feasibility of quantifying ecosystem-atmosphere $C^{18}O^{16}O$ exchange using laser spectroscopy and the flux-gradient method, *Agric. For. Meteorol.*, *135*(1–4), 44–60.

Griffis, T. J., J. Zhang, J. M. Baker, N. Kljun, and K. Billmark (2007), Determining carbon isotope signatures from micrometeorological measurements: Implications for studying biosphere-atmosphere exchange processes, *Boundary Layer Meteorol.*, *123*(2), 295–316.

Griffis, T. J., S. D. Sargent, J. M. Baker, X. Lee, B. D. Tanner, J. Greene, E. Swiatek, and K. Billmark (2008), Direct measurement of biosphere-atmosphere isotopic CO_2 exchange using the eddy covariance technique, *J. Geophys. Res.*, *113*, D08304, doi:10.1029/2007JD009297.

Griffis, T., J. Baker, S. Sargent, M. Erickson, J. Corcoran, M. Chen, and K. Billmark (2010a), Influence of C_4 vegetation on $^{13}CO_2$ discrimination and isoforcing in the upper Midwest, United States, *Global Biogeochem. Cycles*, *24*, GB4006, doi:10.1029/2009GB003768.

Griffis, T., et al. (2010b), Determining the oxygen isotope composition of evapotranspiration using eddy covariance, *Boundary Layer Meteorol.*, *137*, 307–326, doi:10.1007/s10546-010-9529-5.

Harwood, K., J. Gillon, H. Griffiths, and M. Broadmeadow (1998), Diurnal variation of $\Delta^{13}CO_2$, $\Delta C^{18}O^{16}O$ and evaporative site enrichment of δH_2O in Piper aduncum under field conditions in Trinidad, *Plant Cell Environ.*, *21*(3), 269–283.

Hatch, M., and J. Burnell (1990), Carbonic anhydrase activity in leaves and its role in the first step of C_4 photosynthesis, *Plant Physiol.*, *93*, 825–828.

He, H., and R. Smith (1999), Stable isotope composition of water vapor in the atmospheric boundary layer above the forests of New England, *J. Geophys. Res.*, *104*, 11,657–11,673.

Hesterburg, R., and U. Siegenthaler (1991), Production and stable isotopic composition of CO_2 in soil near Bern, Switzerland, *Tellus, Ser. B*, *43*, 197–205.

Ishizawa, M., T. Nakazawa, and K. Higuchi (2002), A multi-box model study of the role of the biospheric metabolism in the recent decline of $\delta^{18}O$ in atmospheric CO_2, *Tellus, Ser. B*, *54*, 307–324.

Lai, C. T., J. R. Ehleringer, B. J. Bond, and K. T. Paw U (2006a), Contributions of evaporation, isotopic non-steady state transpiration and atmospheric mixing on the delta O-18 of water vapour in Pacific Northwest coniferous forests, *Plant Cell Environ.*, *29*(1), 77–94.

Lai, C. T., A. J. Schauer, C. Owensby, J. M. Ham, B. Helliker, P. P. Tans, and J. R. Ehleringer (2006b), Regional CO_2 fluxes inferred from mixing ratio measurements: estimates from flask air samples in central Kansas, USA, *Tellus, Ser. B*, *58*(5), 523–536.

Lee, H., R. Smith, and J. Williams (2006), Water vapour O-18/O-16 isotope ratio in surface air in New England, USA, *Tellus, Ser. B*, *58*(4), 293–304.

Lee, X., S. Sargent, R. Smith, and B. Tanner (2005), In-situ measurement of the water vapor $^{18}O/^{16}O$ isotope ratio for atmospheric and ecological applications, *J. Atmos. Oceanic Technol.*, *22*, 555–565.

Lee, X., T. Griffis, J. Baker, K. Billmark, K. Kim, and L. Welp (2009), Canopy-scale kinetic fractionation of atmospheric carbon dioxide and water vapor isotopes, *Global Biogeochem. Cycles*, *23*, GB1002, doi:10.1029/2008GB003331.

Lee, X. H., K. Kim, and R. Smith (2007), Temporal variations of the $^{18}O/^{16}O$ signal of the whole-canopy transpiration in a temperate forest, *Global Biogeochem. Cycles*, *21*(3), GB3013, doi:10.1029/2006GB002871.

Leroux, X., T. Bariac, and A. Mariotti (1995), Spatial partitioning of the soil-water resource between grass and shrub components in a West-African humid Savanna, *Oecologia*, *104*(2), 147–155.

Lis, G., L. I. Wassenaar, and M. J. Hendry (2008), High-precision laser spectroscopy D/H and O-18/O-16 measurements of microliter natural water samples, *Anal. Chem.*, *80*(1), 287–293, doi:10.1021/ac701716q.

Majoube, M. (1971), Fractionnement en oxygene-18 et en deuterium entre l'eau et sa vapeur, *J. Chim. Phys.*, *68*, 1423–1436.

Makino, A., H. Sakashita, J. Hidema, T. Mae, K. Ojima, and B. Osmond (1992), Distinctive responses of ribulose-1,5-bisphosphate carboxylase and carbonic anhydrase in wheat leaves to nitrogen nutrition and their possible relationship to CO_2 transfer resistance, *Plant Physiol.*, *100*, 1737–1743.

Mills, G., and H. Urey (1940), The kinetics of isotopic exchange between carbon dioxide, bicarbonate ion and water, *J. Am. Chem. Soc.*, *62*, 1019–1026.

Nickerson, N., and D. Risk (2009), A numerical evaluation of chamber methodologies used in measuring the delta C-13 of soil respiration, *Rapid Commun. Mass Spectrom.*, *23*(17), 2802–2810, doi:10.1002/rcm.4189.

Ogée, J., P. Peylin, M. Cuntz, T. Bariac, Y. Brunet, P. Berbigier, P. Richard, and P. Ciais (2004), Partitioning net ecosystem carbon exchange into net assimilation and respiration with canopy-scale isotopic measurements: An error propagation analysis with $^{13}CO_2$ and $CO^{18}O$ data, *Global Biogeochem. Cycles*, *18*, GB2019, doi:10.1029/2003GB002166.

Powers, H. H., J. E. Hunt, D. T. Hanson, and N. G. McDowell (2010), A dynamic soil chamber system coupled with a tunable diode laser for on-line measurements of delta C-13, delta O-18, and efflux rate of soil-respired CO_2, *Rapid Commun. Mass Spectrom.*, *24*(3), 243–253, doi:10.1002/rcm.4380.

Riley, W. J., C. J. Still, M. S. Torn, and J. A. Berry (2002), A mechanistic model of $H_2^{18}O$ and $C^{18}OO$ fluxes between ecosystems and the atmosphere: Model description and sensitivity analyses, *Global Biogeochem. Cycles*, *16*(4), 1095, doi:10.1029/2002GB001878.

Riley, W. J., C. J. Still, B. R. Helliker, M. Ribas-Carbo, and J. A. Berry (2003), O-18 composition of CO_2 and H_2O ecosystem pools and fluxes in a tallgrass prairie: Simulations and comparisons to measurements, *Global Change Biol.*, *9*(11), 1567–1581.

Seibt, U., L. Wingate, J. Lloyd, and J. A. Berry (2006), Diurnally variable $\delta^{18}O$ signatures of soil CO_2 fluxes indicate carbonic anhydrase activity in a forest soil, *J. Geophys. Res.*, *111*, G04005, doi:10.1029/2006JG000177.

Still, C., W. Riley, B. Helliker, and J. Berry (2005), Simulation of ecosystem $C^{18}OO$ isotope fluxes in a tallgrass prairie: Biological and physical controls, in *Stable Isotopes and Biosphere-Atmosphere Interactions: Processes and Biological Controls*, pp. 154–170, Elsevier, New York.

Still, C. J., et al. (2009), Influence of clouds and diffuse radiation on ecosystem-atmosphere CO_2 and $CO^{18}O$ exchanges, *J. Geophys. Res.*, *114*, G01018, doi:10.1029/2007JG000675.

Tans, P. P. (1998), Oxygen isotopic equilibrium between carbon dioxide and water in soils, *Tellus, Ser. B*, *50*(4), 400–400.

Wang, L., K. Caylor, and D. Dragoni (2009), On the calibration of continuous, high-precision $\delta^{18}O$ and $\delta^{2}H$ measurements using an off-axis integrated cavity output spectrometer, *Rapid Commun. Mass Spectrom.*, *23*, 530–536.

Wang, X., and D. Yakir (1995), Temporal and spatial variations in the oxygen-18 content of leaf water in different plant species, *Plant Cell Environ.*, *18*(12), 1377–1385.

Welker, J. (2000), Isotopic (delta O-18) characteristics of weekly precipitation collected across the USA: An initial analysis with application to water source studies, *Hydrol. Processes*, *14*(8), 1449–1464.

Welp, L. R., X. Lee, K. Kim, T. J. Griffis, K. A. Billmark, and J. M. Baker (2008), $\delta^{18}O$ of water vapour, evapotranspiration and the sites of leaf water evaporation in a soybean canopy, *Plant Cell Environ.*, *31*(9), 1214–1228, doi:10.1111/j.1365-3040.2008.01826.x.

Wen, X.-F., X.-M. Sun, S.-C. Zhang, G.-R. Yu, S. D. Sargent, and X. Lee (2008), Continuous measurement of water vapor D/H and O-18/O-16 isotope ratios in the atmosphere, *J. Hydrol.*, *349*(3–4), 489–500, doi:10.1016/j.jhydrol.2007.11.021.

Wingate, L., U. Seibt, K. Maseyk, J. Ogée, P. Almeida, D. Yakir, J. S. Pereira, and M. Mencuccini (2008), Evaporation and carbonic anhydrase activity recorded in oxygen isotope signatures of net CO_2 fluxes from a Mediterranean soil, *Global Change Biol.*, *14*(9), 2178–2193, doi:10.1111/j.1365-2486.2008.01635.x.

Wingate, L., et al. (2009), The impact of soil microorganisms on the global budget of delta O-18 in atmospheric CO_2, *Proc. Natl. Acad. Sci. U. S. A.*, *106*(52), 22,411–22,415, doi:10.1073/pnas.0905210106.

Wingate, L., J. Ogée, R. Burlett, and B. Alexandre (2010), Strong seasonal disequilibrium measured between the oxygen isotope signals of leaf and soil CO_2 exchange, *Global Change Biol.*, *16*(11), 3048–3064, doi:10.1111/j.1365-2486.2010.02186.x.

Xiao, W., X. Lee, T. Griffis, K. Kim, L. Welp, and Q. Yu (2010), A modeling investigation of canopy-air oxygen isotopic exchange of water vapor and carbon dioxide in a soybean field, *J. Geophys. Res.*, *115*, G01004, doi:10.1029/2009JG001163.

Yakir, D. (2003), The stable isotopic composition of atmospheric CO_2, in *The Atmosphere, Treatise on Geochemistry*, vol. 4, edited by H. D. Holland and K. K. Turekian, chap. 4.07, pp. 175–212, Elsevier, Oxford, U. K.

Yakir, D., and L. D. L. Sternberg (2000), The use of stable isotopes to study ecosystem gas exchange, *Oecologia*, *123*(3), 297–311.

Yakir, D., and X. F. Wang (1996), Fluxes of CO_2 and water between terrestrial vegetation and the atmosphere estimated from isotope measurements, *Nature*, *380*(6574), 515–517.

Zhang, J., T. J. Griffis, and J. M. Baker (2006), Using continuous stable isotope measurements to partition net ecosystem CO_2 exchange, *Plant Cell Environ.*, *29*(4), 483–496.

Zobitz, J. M., S. P. Burns, M. Reichstein, and D. R. Bowling (2008), Partitioning net ecosystem carbon exchange and the carbon isotopic disequilibrium in a subalpine forest, *Global Change Biol.*, *14*(8), 1785–1800, doi:10.1111/j.1365-2486.2008.01609.x.

J. M. Baker, Agricultural Research Service, U.S. Department of Agriculture, Saint Paul, MN 55108, USA.

K. Billmark, M. Erickson, J. Fassbinder, T. J. Griffis, and N. Schultz, Department of Soil, Water, and Climate, University of Minnesota, Saint Paul, MN 55108, USA. (tgriffis@umn.edu)

N. Hu and W. Xiao, School of Applied Meteorology, Nanjing University of Information Science and Technology, Nanjing, Jiangsu 210044, China.

X. Lee and X. Zhang, School of Forestry and Environmental Studies, Yale University, New Haven, CT 06511, USA.